The Improvement in Wear Resistance of Ion Implanted Materials

Stephen E. Harding B.A. (Oxon)

MSc Dissertation
AERE Harwell/ Brighton Polytechnic
1977

B R I G H T O N P O L Y T E C H N I C

Department of Applied Physics

M.Sc. Degree in Applied Solid State Physics

Dissertation

by

Stephen E. Harding B.A.(Oxon)

The Improvement In Wear Resistance of Ion Implanted Materials

AERE Harwell, 1977

Abstract

Studies have been made on the wear properties of various ion implanted steel discs in relation to the nature of the steel, the ion species implanted and prior heat treatment. A comparison with the more conventional methods of wear improvement, i.e. heat treating or alloying, has also been made together with an attempt to supplement already existing ideas (which are reviewed) as to why, from a molecular point of view, wear properties should be improved by ion implantation.

Contents

1. Introduction

Ion implantation has been used for several years as an accurate method of doping semiconductors. However, it is only recently that it has been used as a method for increasing the resistance to wear of two materials in contact and moving relative to each other. It has the advantage over other methods of improving wear properties - for example heat treating and alloying - in that, firstly, there is no change in the bulk properties or dimensions of the treated sample. Secondly, materials that are too expensive for bulk use may be acceptable in the quantities needed for surface implantation. The treated surface region remains integral with the bulk material so no bonding or interface problems arise. The implantation process is carried out at room temperature so there is no degradation or size change due to heating as occurs in diffusion processes and finally, as the process does not lead to any dimensional changes, it can be used on already finished articles.

In this study, the effect of nitrogen ion implantation on stainless steel, tool steel, nitriding steel and plain carbon steel was investigated using the "pin on disc" wear test. A steel disc is made to rotate against a steel pin under load. The pin was unimplanted stainless steel except for the "like pin on like disc" tests (see section 3.1). Supplementary studies were made to compare the effect of nitriding steel with different ion species, i.e. boron, carbon and neon ions, and also to compare the effect of heat treatment as an alternative - and as an addition - to ion implantation. Nuclear reaction analyses were carried out on the N^+ implanted specimens to determine the implanted nitrogen dose and X-ray photoelectron spectroscopy analysis was used to determine the depth profiles of the N^+ and Ne^+ ions. An examination of the wear tracks using talysurf and scanning electron microscopy was made.

2. The Wear of Materials and Radiation Damage

2.1 The Wear of Materials

A potential wear situation exists whenever there is relative motion between two surfaces in contact under load. As both surfaces in a wear couple are generally rough, the actual area of contact is much smaller than the apparent area. The actual area can be estimated either by measuring the contact resistance between the two surfaces, by microscopic observation, or from the flow stress of the material. The regions of contact thus experience a high normal stress and yielding may occur at the local points of contact usually referred to as asperities. Contact areas will weld together and must then be broken to initiate and sustain relative motion. This is referred to as adhesive wear.

Wear debris results as the asperities are broken off and may remain trapped at the sliding interface giving rise to abrasive wear, in which material is removed largely by ploughing.

To reduce wear, one therefore has to reduce the formation of junctions by interposing an intermediate layer; this can be an oxide film (the formation of which is fortunately aided by frictional heating*) or the provision of a liquid lubricant.

Other types of wear can also occur. Fretting results from oscillatory movement between two surfaces, for instance vibrating machine parts. Fatigue wear results from cyclic loading and loss of material occurs by spalling of surface layers. Erosive wear occurs when grit particles impinge on solids. Cavitation erosion can occur when a component rotates in a fluid medium. A full review of the

---

*An oxide film has the following effect: if the junction is weaker than the metals themselves, in the presence of an oxide film shearing will occur at the actual interface where the junction is formed within the oxide and the amount of material removed from either surface will be small.

various types of wear is given in standard texts such as Principles and Applications of Tribology by Moore (Pergamon)[1]. The predominant type of wear depends on the nature of the relative motion (for example sliding or rolling), the material and the lubrication conditions.

2.1.1 Wear Parameters

The following four parameters have been used in tribology.[1,2]

1) Linear wear rate

$$K_L = \frac{\text{thickness of layer removed}}{\text{sliding distance}} = \frac{h}{X} \quad \ldots\ldots (1)$$

2) Volumetric wear rate

$$K_V = \frac{\text{volume of layer removed}}{\text{sliding distance x apparent area}} = \frac{\Delta V}{XA_a} \quad \ldots\ldots (2)$$

3) Gravimetric wear rate

$$K_W = \frac{\text{weight of layer removed}}{\text{sliding distance x apparent area}} = \frac{\Delta W}{XA_a} \quad \ldots\ldots (3)$$

4) Pin wear paremeter

$$K_P = \frac{3 \text{ x hardness x volume of layer removed}}{\text{sliding distance x load}} = \frac{3H\Delta V}{XL} \quad \ldots\ldots (4)$$

In these experiments, the volumetric wear rate K_V was chosen as the most suitable parameter because it takes into account the change in apparent area of contact. K_W measures much the same thing as it differs only by a density factor, whereas K_P takes into account change in hardness and load. However, since most of the tests were done at constant load (10N) and hardness changes were negligible, K_V was used.

2.1.2 Wear curves

Wear measurements were made using an Avery Denison T62 pin and disc machine, a fuller description of which is given in

section 3.6. If the total volume loss from the pin is plotted against total sliding distance a characteristic curve is obtained as in Fig. 1. The point 0 is the start of the wear run and the volume loss is initially curvilinear (0 → X). This is the "running in" wear region, essentially adhesive wear. Eventually a steady state wear region is attained (X → Y) providing the load and speed are kept constant. In this region, the asperities have been smoothed out and the wear process is more uniform. Close examination was made of data from the steady state wear region and presented as plots of volumetric wear rate against incremental sliding distance.

2.2 Ion Induced Radiation Damage

High energy ions implanted into a material lose energy through elastic and inelastic (electron excitation) collisions, largely through the former process. The net effect is to produce an ion range which is Gaussian, although this will be distorted due to sputtering, oxide films and other non uniformities. The amount of sputtering depends on the material, the ion and the energy and this is considered in the discussion at the end of this study.

Typical damage caused to the surface region is illustrated by Fig. 3. Atoms are displaced creating interstitials and vacancies and the former generally migrate to dislocations or to the surface leaving a depleted zone. It would appear at first that such severe disruption of the surface would render it amorphous - and this is generally true for non-metallic targets - but metals are generally very resistant due to the fact that the interatomic forces are not well directed and are relatively short range. A dislocation network arises instead and so ion implantation has the effect of work hardening the surface of the

metal. An increase in strain energy is associated with the defect formation, and if in addition, an excess quantity of interstitial atoms which stabilize as intermetallic compounds (for example iron nitrides, borides and carbides) can be injected into a metal, then a macroscopic stress may be produced around the region of damage i.e. the implantation profile.[3] This compressive stress results because the material, when bombarded, tries to expand, but is constrained by the rest of the substrate (Fig. 4).

In 1963 Lindhard, Scharff and Schiøtt[4] calculated the ion ranges in certain materials for various ion species. By knowing the interatomic potential (assumed to be Thomas-Fermi), it is possible to calculate the average rate of energy loss. After introducing certain semi-empirical approximations a universal curve for the elastic stopping in terms of reduced energy and range parameters was then obtained. However, the effect of ion implantation in improving wear properties extended to regions far beyond that predicted by LSS theory and so it has been postulated that there is an increase in diffusivity under the influence of a compressive stress.

3. Experimental Procedure

3.1 The Steels used

The steel discs used in this study were: stainless steel (En 58B), tool steel (N.S.O.H.), nitriding steel (En 40B) and carbon steel (En8)*. Stainless steels are used for both corrosion and heat resistance applications. The corrosion resistance is due to a thin oxide film of chromium, or nickel, oxide. En58B (stabilized austenitic chromium nickel steel) contains 18% chromium and 8% nickel.

---

*The nomenclature used here is that of the British Standards Institution.

The term "tool steel" is usually given to high quality special steels used for cutting or forming purposes. All have been shown by previous tests to have good wear resistance. N.S.O.H. (non-shrinking oil hardening) tool steel possesses excellent dimensional stability with freedom from distortion and cracking in heat treatment. Their properties are influenced strongly by undissolved carbon precipitates.

Nitriding steels contain one or more of the major nitride forming elements (Al, Cr and Mo), although at suitable temperatures and with the proper atmosphere, all steels are capable of producing iron nitrides.

Carbon steels are unalloyed steels containing no deliberately added impurities. En8 is a medium tensile carbon steel used for many automobile and general engineering components. Table 1 gives a comparison of the amounts of carbon, nickel chromium and molybdenum in each steel.

Table 1

Composition of the steels used (%)

	C	Ni	Cr	Mo
En 58B	0.15 max	7 - 10	17 - 20	-
N.S.O.H.	0.85 - 1.00	-	0.40 - 0.60	-
En 40B	0.20 - 0.30	0.40 max	2.90 - 3.50	0.40 - 0.70
En 8	0.35 - 0.40	-	-	-

The pins were mainly stainless steel, but some work was done using tool steel pins run against tool steel discs and also nitriding steel pins run against nitriding steel discs. Most of the work was done with unimplanted stainless steel pins run against unimplanted, implanted and heat treated samples of the above four discs.

3.1.1 Finishing

The steel discs had been ground and lapped to a diameter of (25.4 ± 0.1)mm and to a flatness of 2.5 μm. The ends of the pins were fine ground to a cone angle of (120° ± 10').

3.2 Heat treating

The number of defects in a solid is proportional to the exponential of its absolute temperature. Thus if we increase the temperature to about 800°C the disorder in the bulk of the material will be about $\exp\left(\frac{-\Delta E}{k.1100}\right) \Big/ \exp\left(\frac{-\Delta E}{k.300}\right)^{*}$ = 1.6×10^{12} times that at room temperature. By quenching the material, i.e. cooling it rapidly, this high defect state can be "frozen in" resulting in a higher resistance to plastic flow. The structure, hardness and strength are also dependent on the actual rate of cooling.

Unimplanted tool steel, nitriding steel and carbon steel discs and a nitrogen implanted tool steel disc were heat treated using a carbolite furnace coupled to AEI sorption and ion pumps (Fig. 5). A vacuum of about 10^{-7} torr was obtained in each case. Table 2 indicates the range of temperatures for hardening and tempering for each steel and also the quenching medium.

Table 2
Quenching Data[5]

Steel	Hardening Temp.	Quench Medium	Tempering Temp.
N.S.O.H.	780 - 820°C	OIL	150 - 300°C
En 40B	800 - 910°C	OIL	570 - 700°C
En 8	830 - 860°C	OIL	550 - 660°C

*ΔE is the formation energy (~ 1 eV), k is Boltzmanns constant.

Each sample was maintained at the hardening temperature for fifteen minutes, tempered for another fifteen minutes, quenched in an oil bath and finally cleaned with acetone.

3.3 Wear Testing

Wear measurements were made using an Avery Denison T62 tribotester (Plate 1). This is a "pin and disc" machine where a disc is made to rotate against a pin which has a load applied normally to it. The machine consists of a motor control unit which drives the disc, an auxillary lubricating system and a load unit for applying normal stresses. The pin is mounted on a hinged load bar. The area of contact and the volume loss is determined from the dimensions of the pin flat, the latter from the relation

$$\Delta V = \frac{1}{3} \pi r^3 \tan \theta \qquad \ldots\ldots (5)$$

where ΔV is the volume loss per run, r the radius of the pin flat and θ the cone angle (120°). From this the volumetric wear rate could be calculated (section 2.1.1).

Firstly the pins were run in at 5N load until the flat was a reasonably uniform circular area (about 0.2mm diameter). Then several runs at loads of either 10N or 40N were made until a flat diameter of about 0.5mm was reached (so that the area of contact for each run was equivalent). On each disc several wear tracks were made corresponding to 10N or 40N or running in.

Since it is the relative wear of implanted and unimplanted discs that we are concerned with then it might at first appear strange measuring the change in geometry of the pins and not the discs. Objections against pin rather than disc measurements would be valid if either component was infinitely hard in which case all the wear would occur in the other component. However this is never the case. The

wear of a given material, say A, against another, B, depends on the nature of B. Thus if another material, C, is worn against B under the same conditions, then the wear properties of A and C can be justifiably compared. In these experiments B represents the pins and A and C the discs.

In these wear tests we use two components of similar hardness [D.P.N. number (350 $\pm$ 60)] so that measurable amounts of wear can be made from the pins.

After wear testing, the discs were talysurfed, from which information as to the main type of wear process occurring in a given wear track could be obtained.

3.4 Surface Topography Measurements

The talysurf (Fig. 6) consists of a stylus moving across the surface of a given material - i.e. in this case, a worn steel disc. (A full description of this apparatus is given in Sakar "Wear of Metals"[2]). The stylus detects a change in the air gap between it and the surface, and the mechanical displacement of the armature is converted into an electrical signal. The surface undulation is finally traced by the pen recorder.

The topography of the surface was also investigated using scanning electron microscopy to look at the wear tracks.

3.5 Ion Implantation Procedure

The steel discs were implanted on one side only using a 120 keV ion accelerator with an oscillating electron gun as the ion source (Fig. 7). When an electric potential (about 6 kV) is applied between the 2 anode wires and the enclosing cathode chamber the thermal electrons in the gas are attracted towards the anodes, drawn through the gap between them and oscillate. This gives rise to long electron paths in

the chamber which increases the chance of cascading (i.e. the formation of secondary and tertiary etc. electrons) - and a figure-of-eight plasma region results. The gaseous positive ions created in this process are attracted out through the slit, accelerated towards and through the extraction electrode and then strike the target. The doses implanted can be estimated from the beam current, but more accurate values can be obtained by the method of nuclear reaction analysis. Previous work by Hartley[6] has shown that the optimum dose for implanting nitrogen ions into En40B nitriding steel is between 2 and 4×10^{17} ions/cm^2. Also from an equation derived by Betts[7] it can be shown that the maximum dose for the energy used in implantations is between 5 and 6×10^{17}; all the excess ions above this dose are lost through sputtering. Thus doses of between 2 and 4×10^{17} ions/cm^2 were aimed at (see Appendix, and Fig. 8).

3.6 Nuclear Reaction Analysis

By using the $^{14}N(d,\alpha)^{12}C$ nuclear reaction, the amount of nitrogen implanted into the specimens could be determined from the emitted α-particle energy spectrum. (Figs. 9 and 10). The reaction is:

$$^{14}_{7}N + ^{2}_{1}H \rightarrow ^{16}_{8}O^{*} \rightarrow ^{12}_{6}C + ^{4}_{2}He + \gamma + Q. \qquad \ldots\ldots (6)$$

where Q is the energy released during the reaction and the $^{16}_{8}O^{*}$ is in a metastable state.

The samples were bombarded with 2.4 MeV deuterons using a Van de Graaff accelerator. The dose of deuterons was monitored using a preset scalar so that each sample could be exposed to a fixed charge of analysing beam.

This method is very useful in determining how much of the implanted species was lost through sputtering, which is discussed later on, but cannot give information about the chemical state of the nitrogen - i.e.

whether it is free, nitrated, nitrited - and for this reason the nuclear reaction data were supplemented by X-ray photoelectron spectroscopy.

3.7 X-ray Photoelectron Spectroscopy (XPS)

Besides giving chemical information about the implanted nitrogen, XPS yielded significant data relating to depth profiles of the implanted nitrogen and neon.

XPS is one of the range of techniques known as electron spectroscopy for chemical analysis (ESCA). A soft X-ray photon of known energy ($h\nu$) impinges on the surface and emits an electron from the inner atomic level. The analysis of the kinetic energies is made in a spectrometer which will have an effective work function $e\phi$ to be overcome by the photoelectron at the entrance slit. The energy measured by the spectrometer is

$$E_{KIN} = h\nu - E_B - e\phi \qquad \ldots\ldots (7)$$

where E_B is the binding energy of an electron in a core level of the surface atom. It is usually only a fraction of an eV wide (for Al K_α lines, 1486.6 eV, the width is about 1.12 eV). The available energy resolution is sufficient to record shifts in E_B due to chemical interaction (about 2 eV for nitriding).

Analyses were possible at various depths by first eroding the sample using argon ions to a given depth and then performing the analysis. After there was only a very small signal for the nitrogen or neon, the analysis was stopped (6000Å for N^+, 300Å for Ne^+) (Figs. 11 to 13).

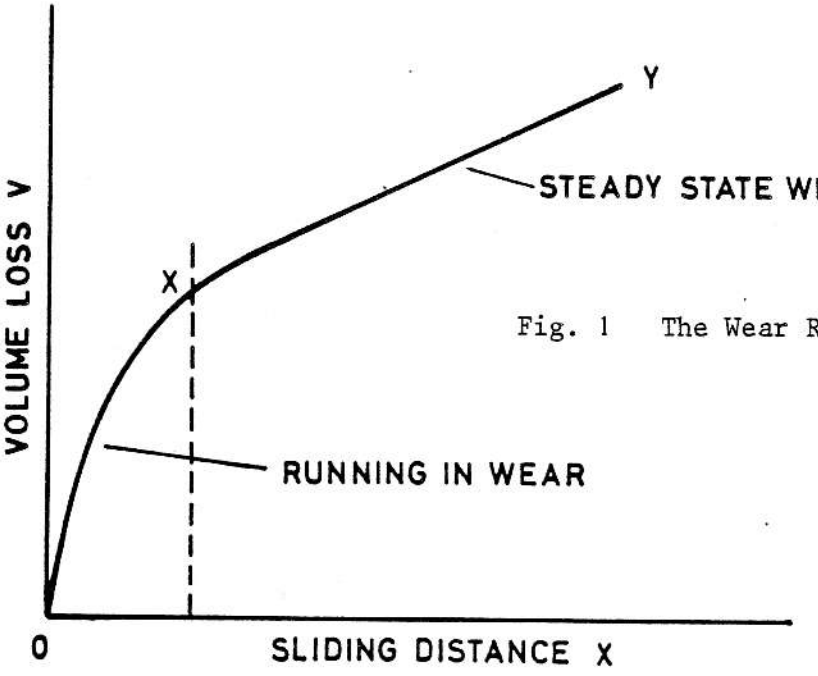

Fig. 1 The Wear Regimes.

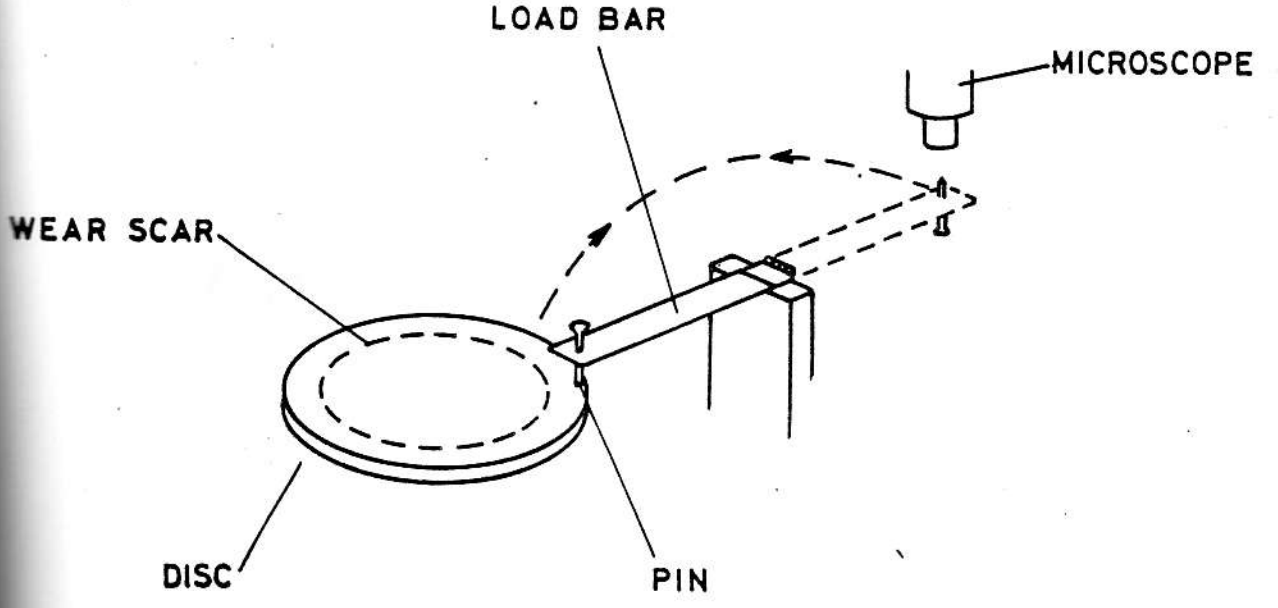

Fig. 2 Pin and disc machine (schematic). The load bar is swung through 180° (broken line) to measure the wear scar under the microscope.

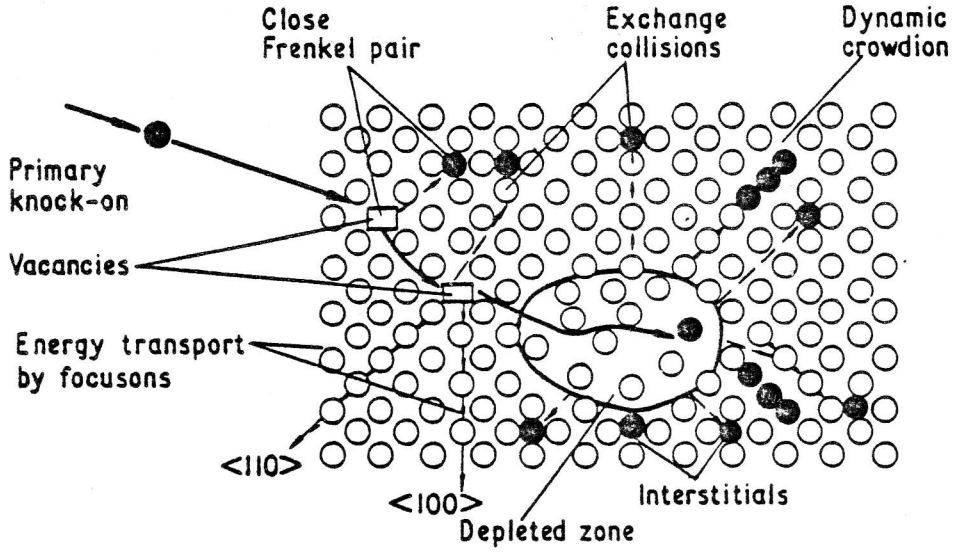

Fig. 3 Defect structures produced during ion bombardment of crystalline or polycrystalline materials.

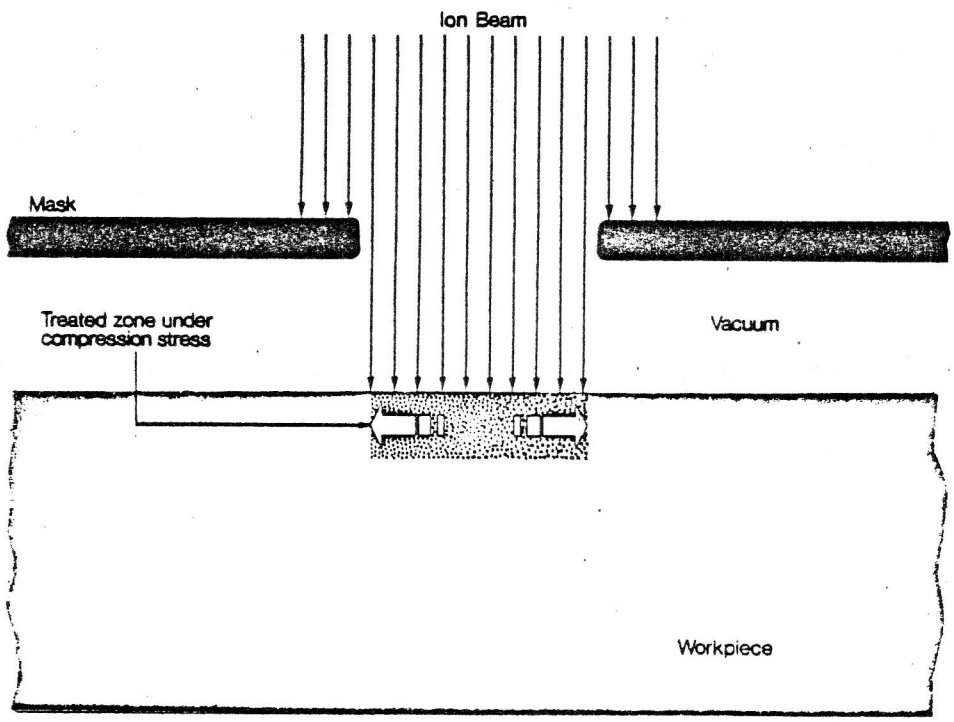

Fig. 4 Ion bombardment will generate a biaxial compressive stress in the surface due to defect formation.

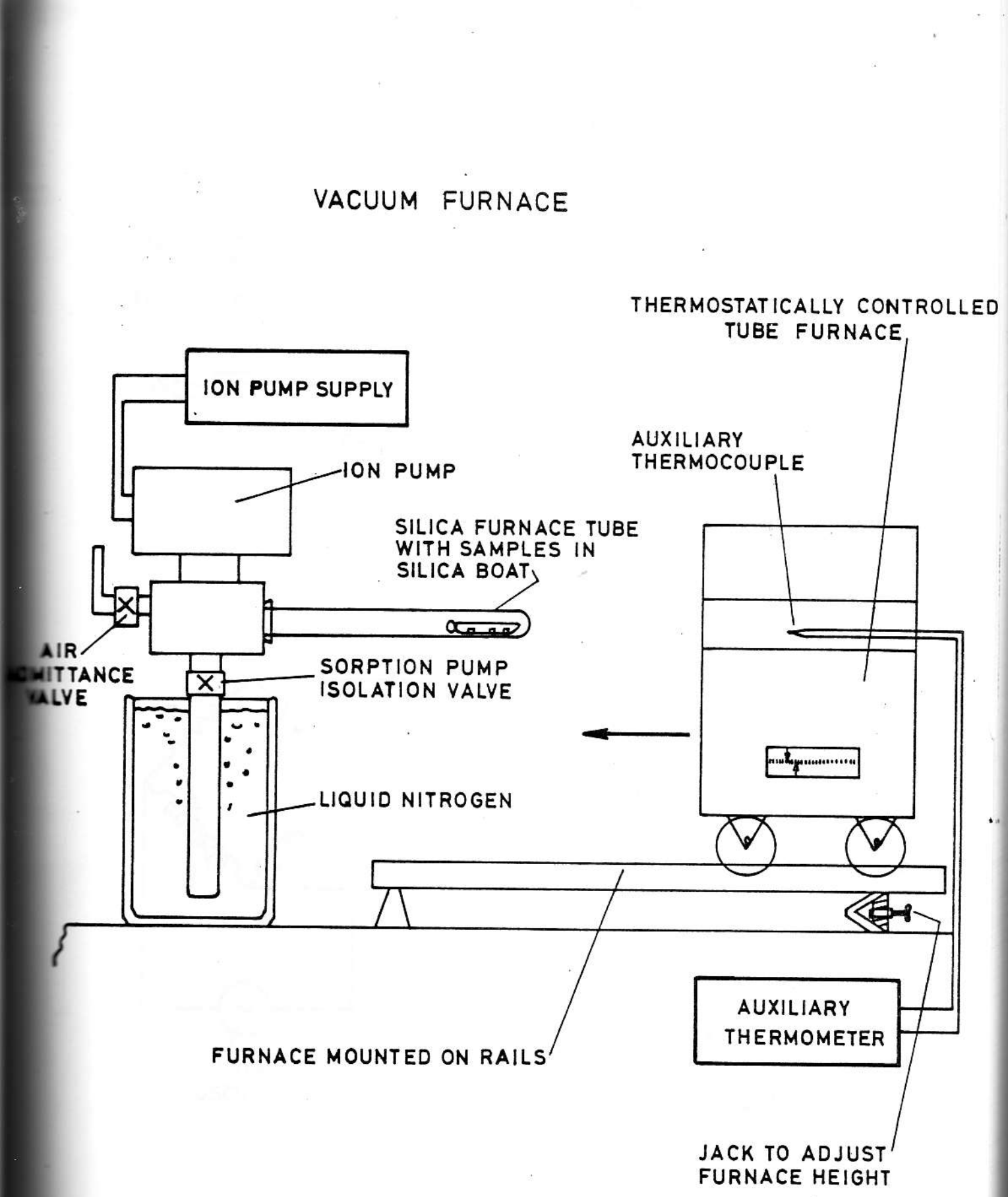

Fig. 5 Vacuum furnace.

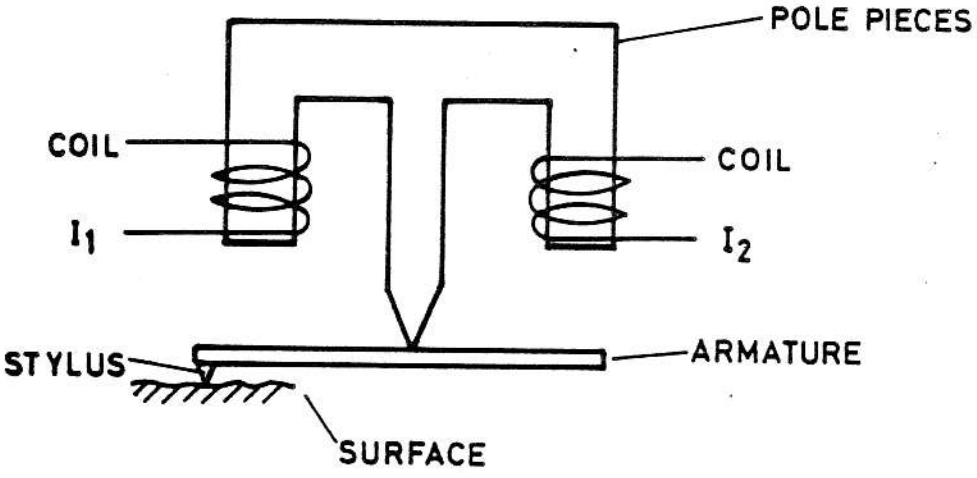

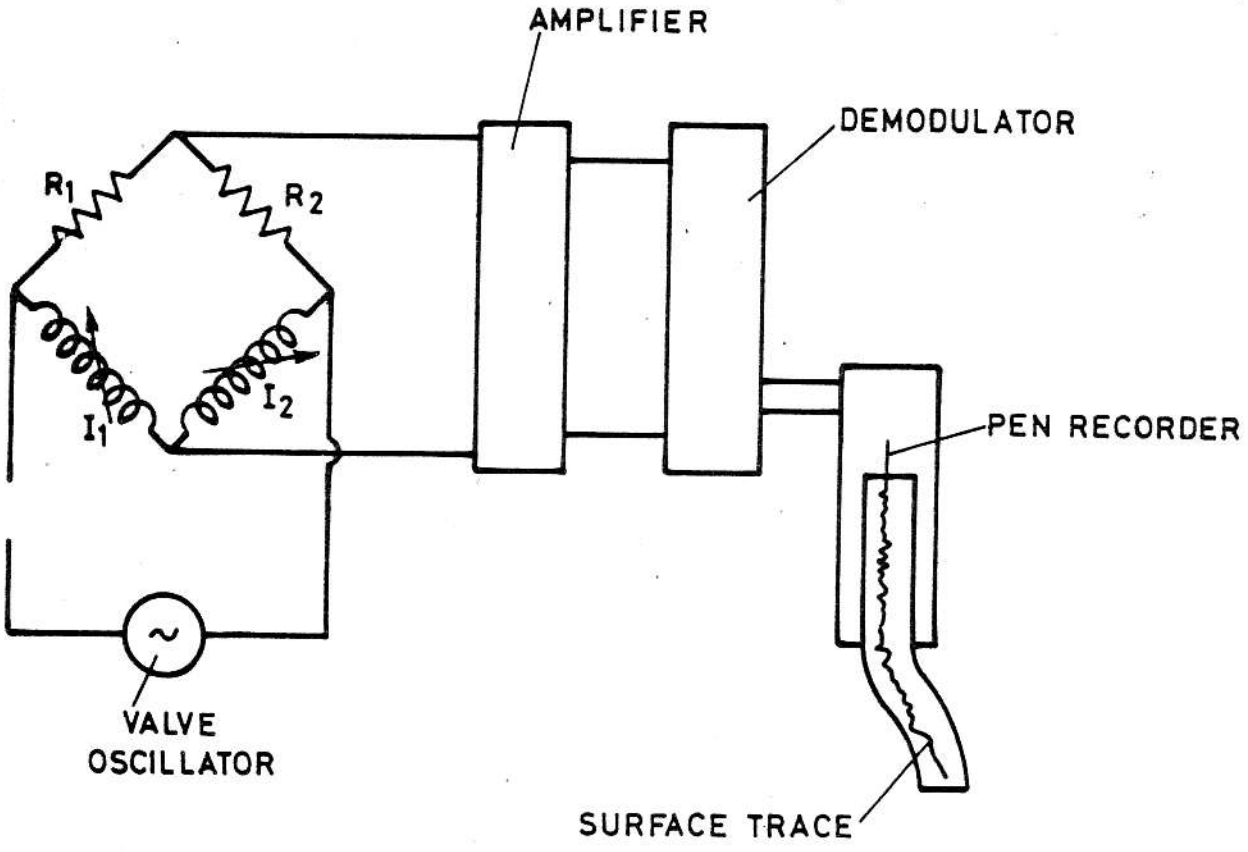

Fig. 6 Principles of a talysurf.[2]

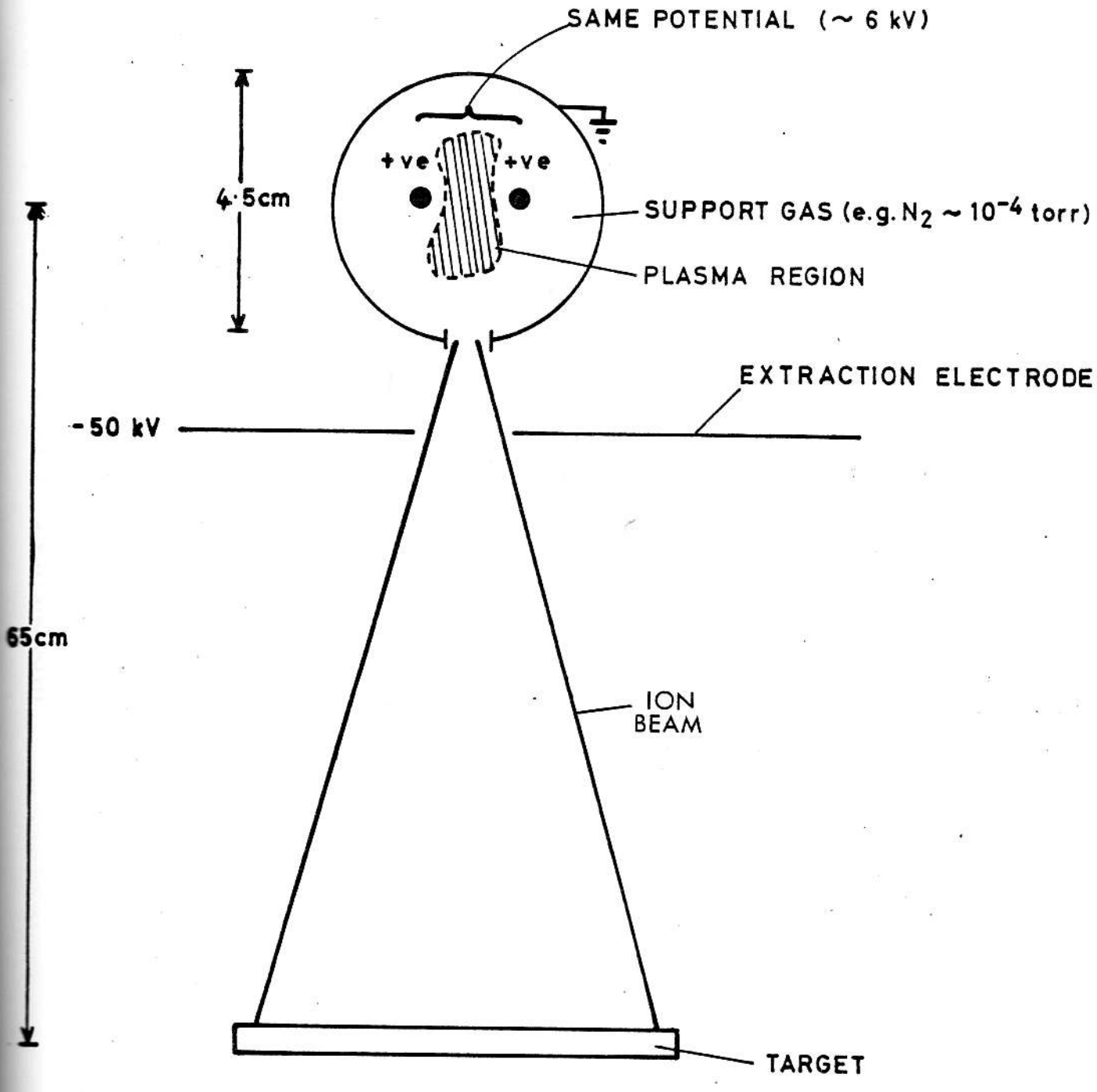

Fig. 7 Principle of the oscillating electron ion source.

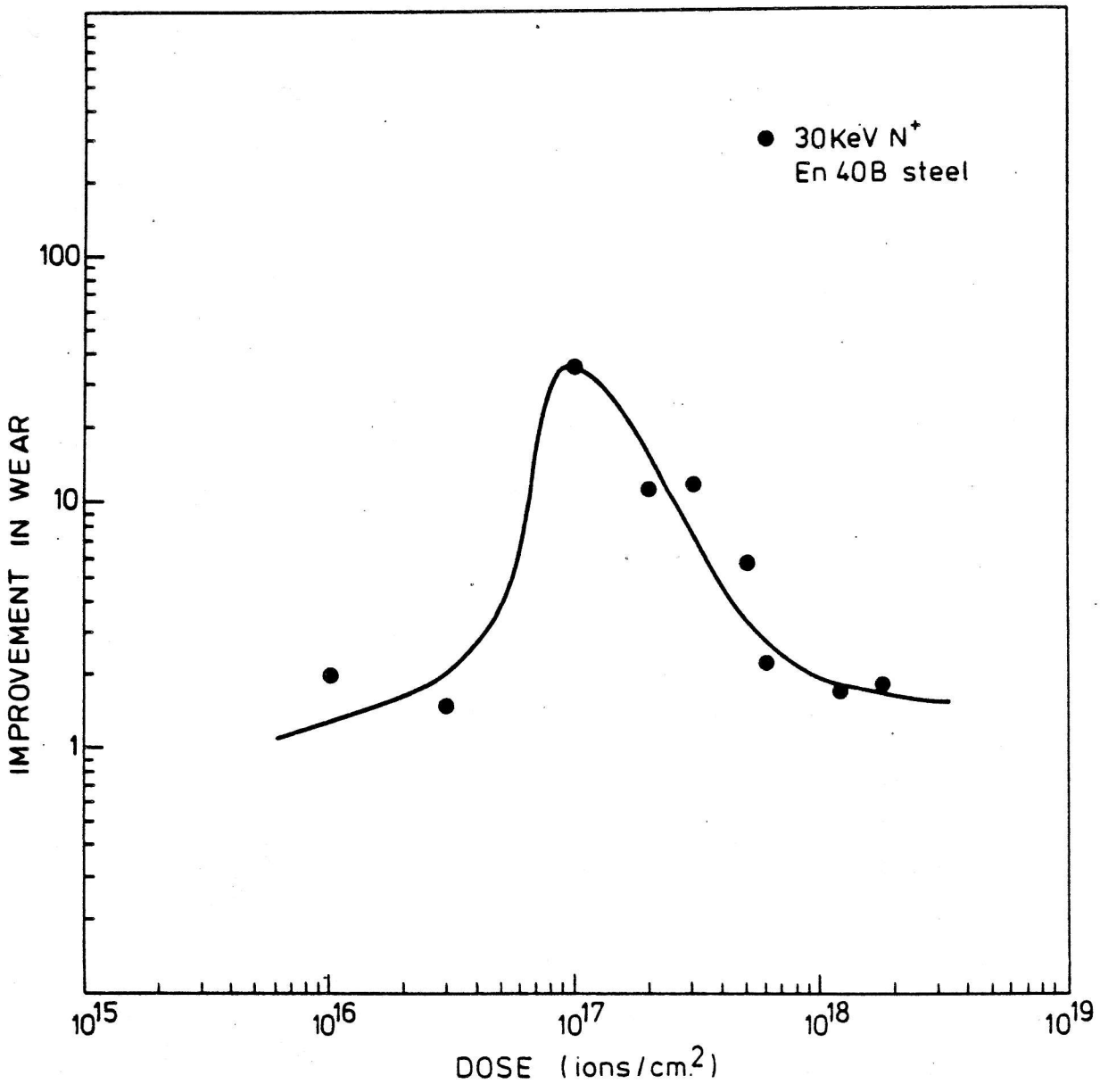

Fig. 8 The relative improvement in wear for the mean of several tests at 10 and 15N load for nitrogen implanted En40B nitriding steel as a function of dose.[6]

4. Results

Captions to the figures and plates

NUCLEAR REACTION ANALYSIS

Fig. 9 : α-particle energy spectrum from the $^{14}N(d,\alpha)^{12}C$ reaction in an N^+ implanted stainless steel disc.

Fig. 10: As for Fig. 9, but with a nitriding steel disc.

DEPTH PROFILES (XPS)

Fig. 11: Depth profile of nitrogen in a nitrogen implanted (5×10^{17} ions/cm^2) En58B stainless steel disc relative to other important species.

Fig. 12: As Fig. 11 but nitrogen implanted (2.8×10^{17} ions/cm^2) En40B nitriding steel disc.

Fig. 13: Depth profile of neon in a neon implanted En40B nitriding steel disc.

LIKE DISC ON LIKE PIN TESTS

Fig.14: Change in volumetric wear rate per unit contact area as a function of sliding distance for pin and disc tests for unimplanted En58B stainless steel, En40B nitriding steel, NSOH tool steel and En8 carbon steel discs lubricated with white spirit. Rotational speed = 600 r.p.m.

Fig. 15: As Fig. 14 except with N^+ implanted discs.

Fig. 16: Change in wear parameter K_p as a function of sliding distance for pin and disc tests on 50 keV N^+ stainless steel discs lubricated with white spirit. Rotational speed = 600 r.p.m.

DISC ON STAINLESS STEEL PIN TESTS

Fig. 17: Change in volumetric wear rate per unit contact area as a function of sliding distance for pin and disc tests on unimplanted En58B stainless steel, En40B nitriding steel, NSOH tool steel and En8 carbon steel discs lubricated with white spirit.

Fig. 18: Change in volumetric wear rate as a function of sliding distance for pin and disc tests on a 50 keV N^+ implanted En58B stainless steel disc lubricated with white spirit.

Fig. 19: As Fig. 18 but with En40B nitriding steel discs.

Fig. 20: As Fig. 18 but with NSOH tool steel discs.

Fig. 21: As Fig. 18 but with En8 carbon steel discs.

Fig. 22: As Fig. 18 but with 50 keV N^+ implanted, 40 keV C^+ implanted, 40 keV B^+ implanted and 50 keV Ne^+ implanted En40B nitriding steel discs.

TALYSURF PROFILES

Fig. 23: Talysurf profiles of N^+ implanted, wear tested (a) stainless steel, (b) nitriding steel and (c) tool steel discs.

Plate II: Scanning electron micrograph of a run in wear groove. The dimension perpendicular to the wear scars is approximately half the width of the groove.

Plate III: Scanning electron micrograph of a wear groove after several runs at 40 newtons pin load.

Plate IV: Scanning electron micrograph of a wear groove after an unlubricated run. Note the rounded edges of the platelet caused by high temperature during wearing.

Captions to the wear improvement tables

3. Unimplanted like on like tests (Fig. 14)

4. Like on like tests (Fig. 15)

5. Unimplanted disc on stainless steel pin tests (Fig. 18)

6. En40B nitriding steel disc on stainless steel pin tests (Fig. 18)

7. NSOH tool steel disc on stainless steel pin tests (Fig. 20).

8. En8 carbon steel disc on stainless steel pin tests (Fig. 21).

9. Species dependence tests (Fig. 22).

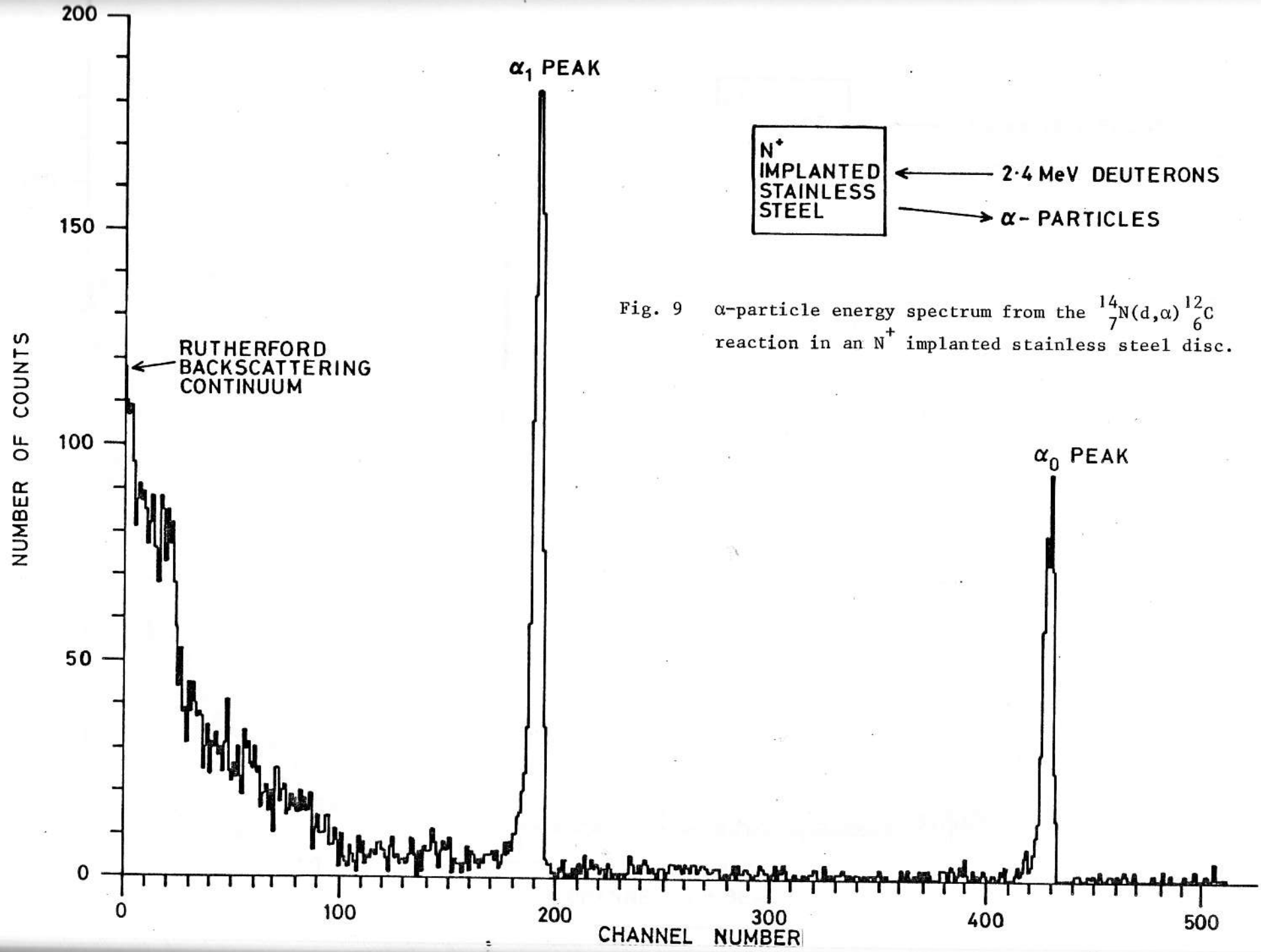

Fig. 9 α-particle energy spectrum from the $^{14}_{7}N(d,\alpha)^{12}_{6}C$ reaction in an N^+ implanted stainless steel disc.

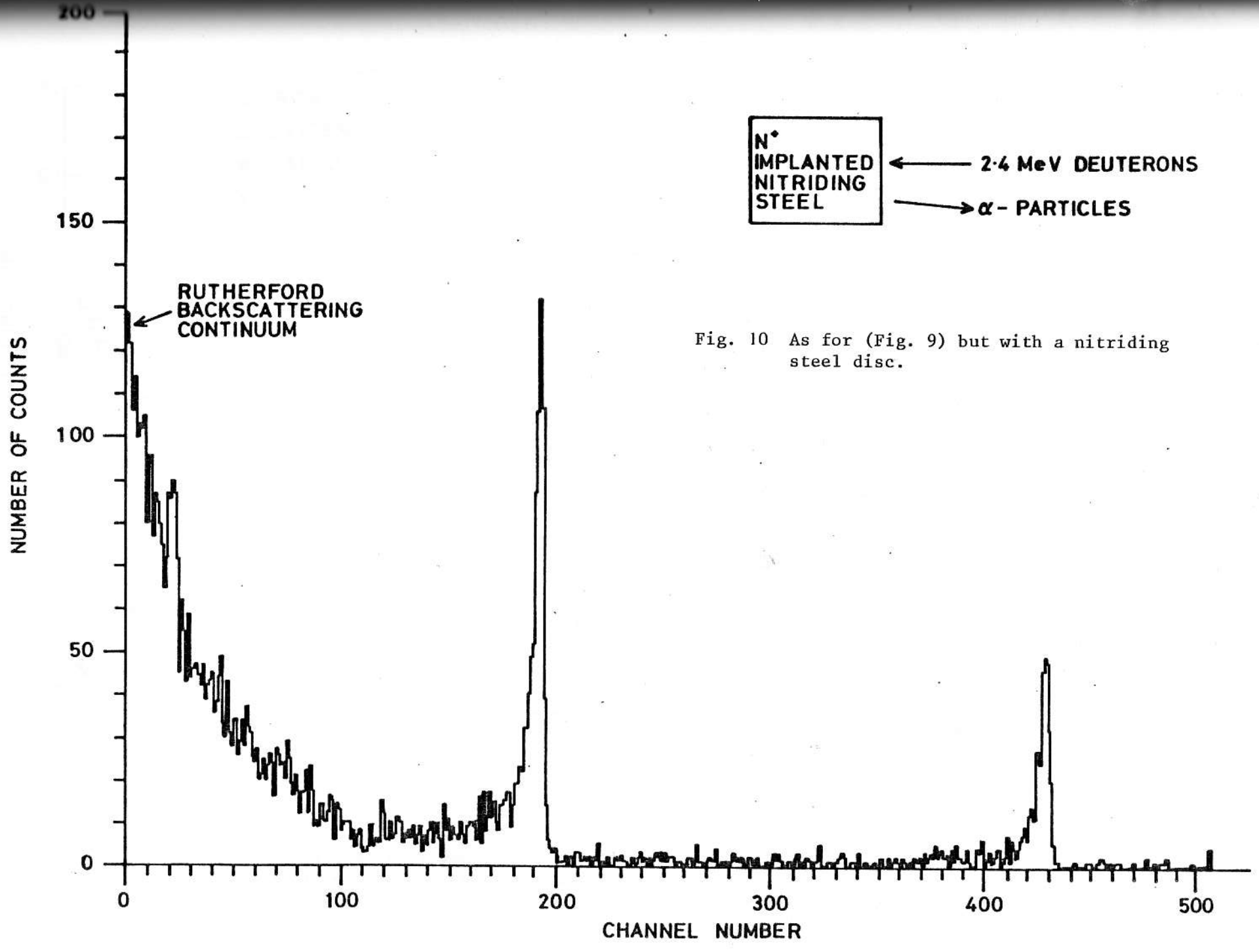

Fig. 10 As for (Fig. 9) but with a nitriding steel disc.

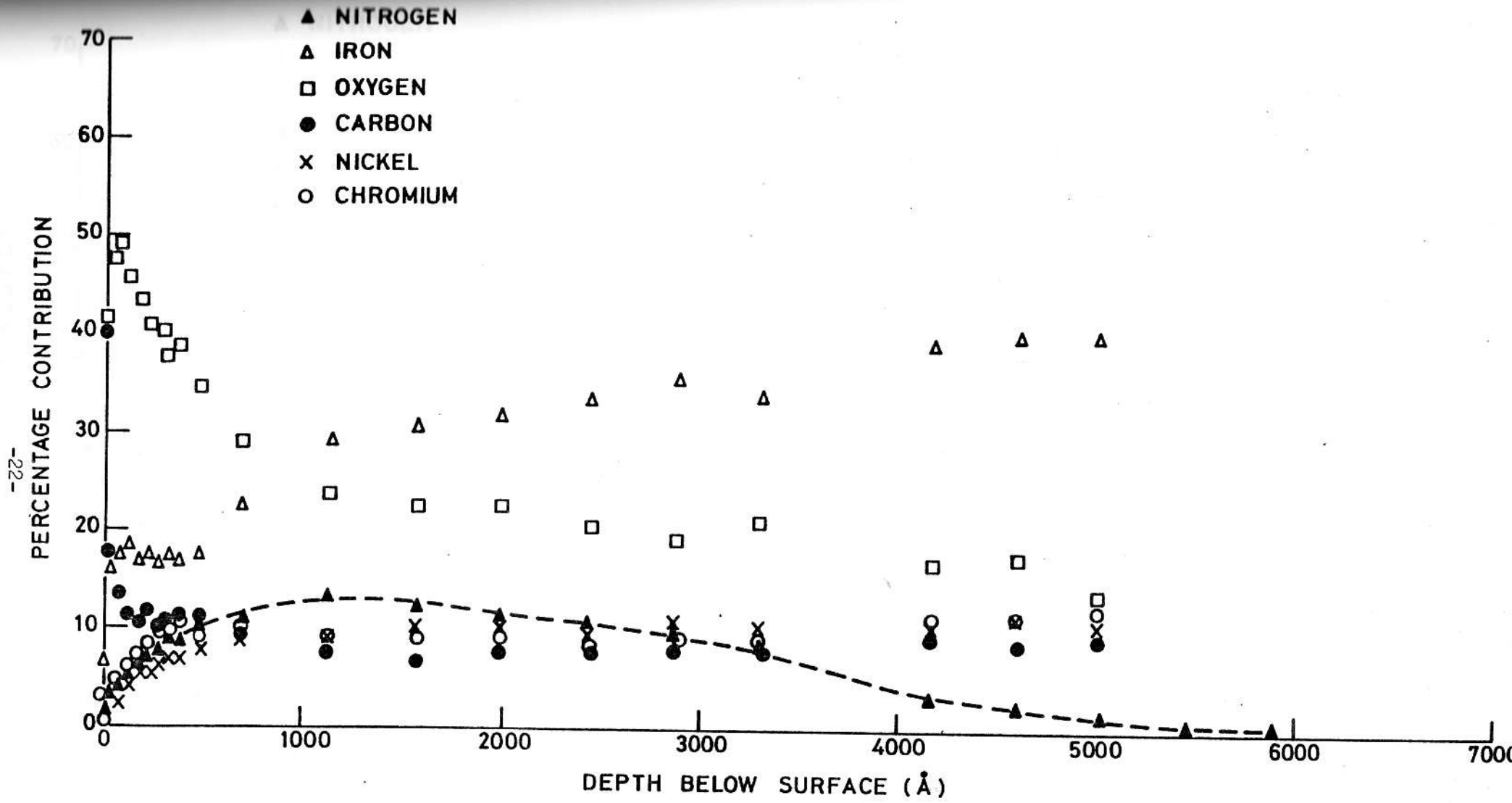

Fig. 11 Depth profile of nitrogen in a nitrogen implanted (5×10^{17} ions/cm^2) En58B stainless steel disc relative to other important species.

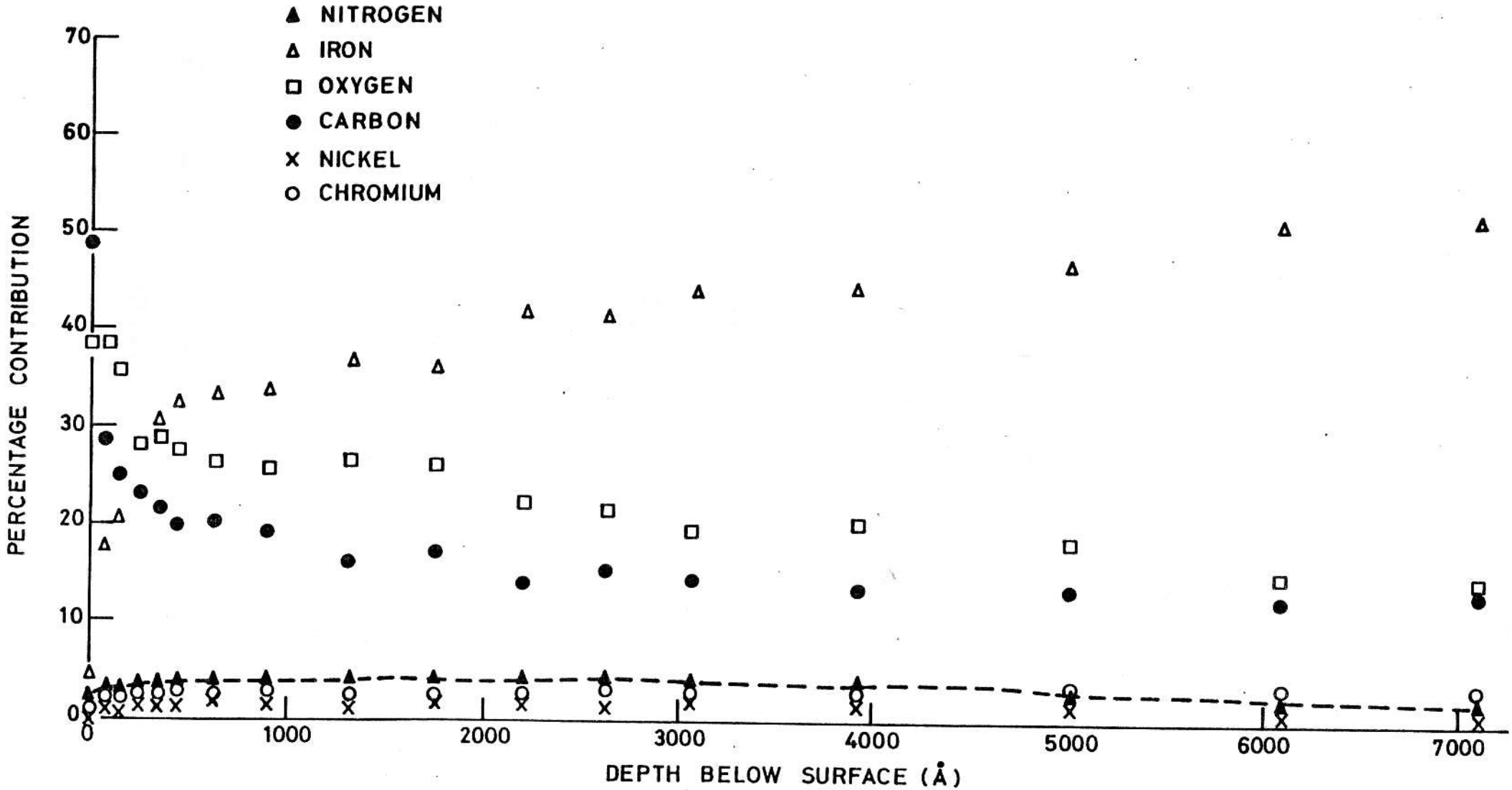

Fig. 12 As Fig. 11 but nitrogen implanted (2.8×10^{17} ions/cm^2) En40B nitriding steel disc.

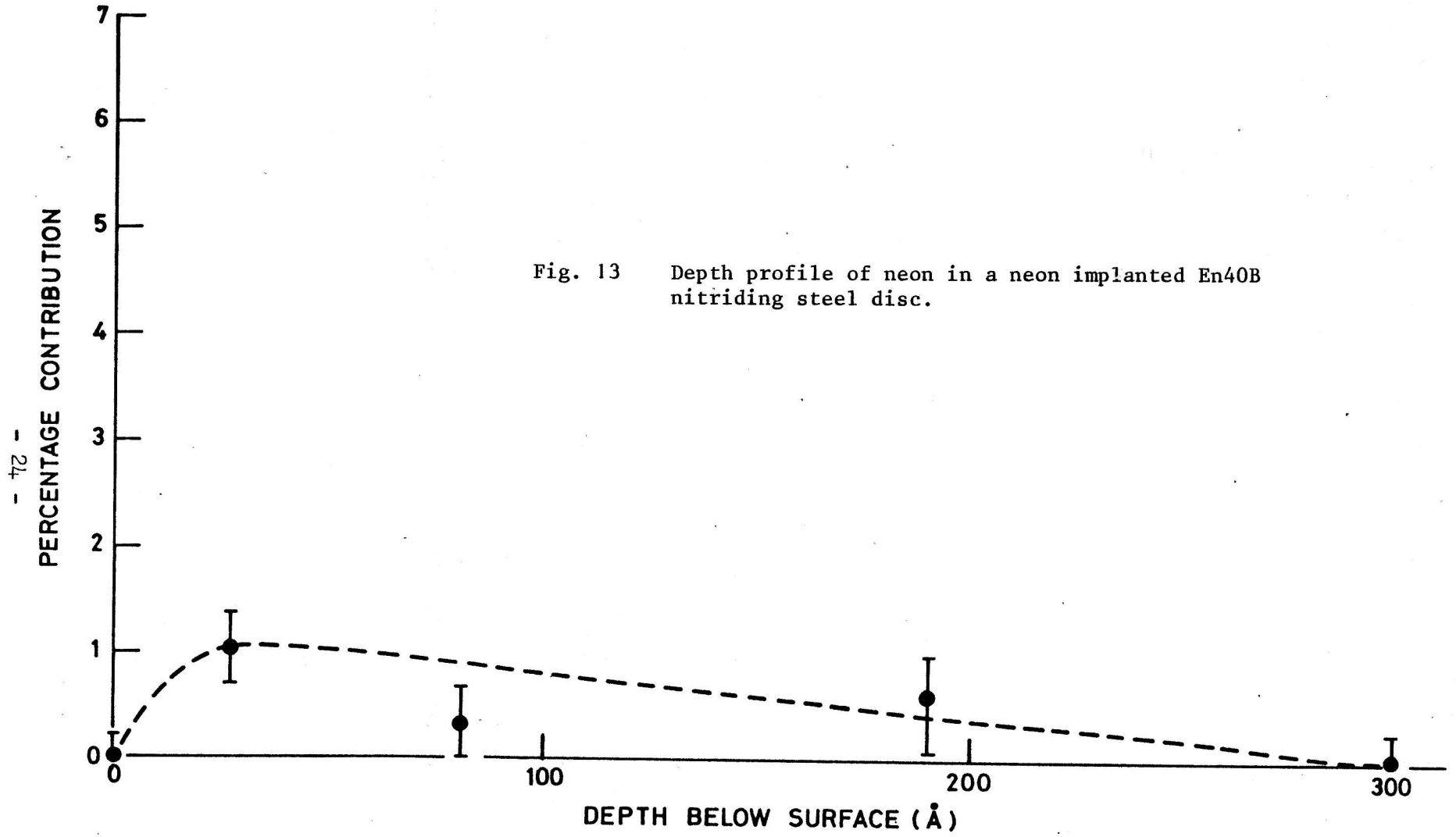

Fig. 13 Depth profile of neon in a neon implanted En40B nitriding steel disc.

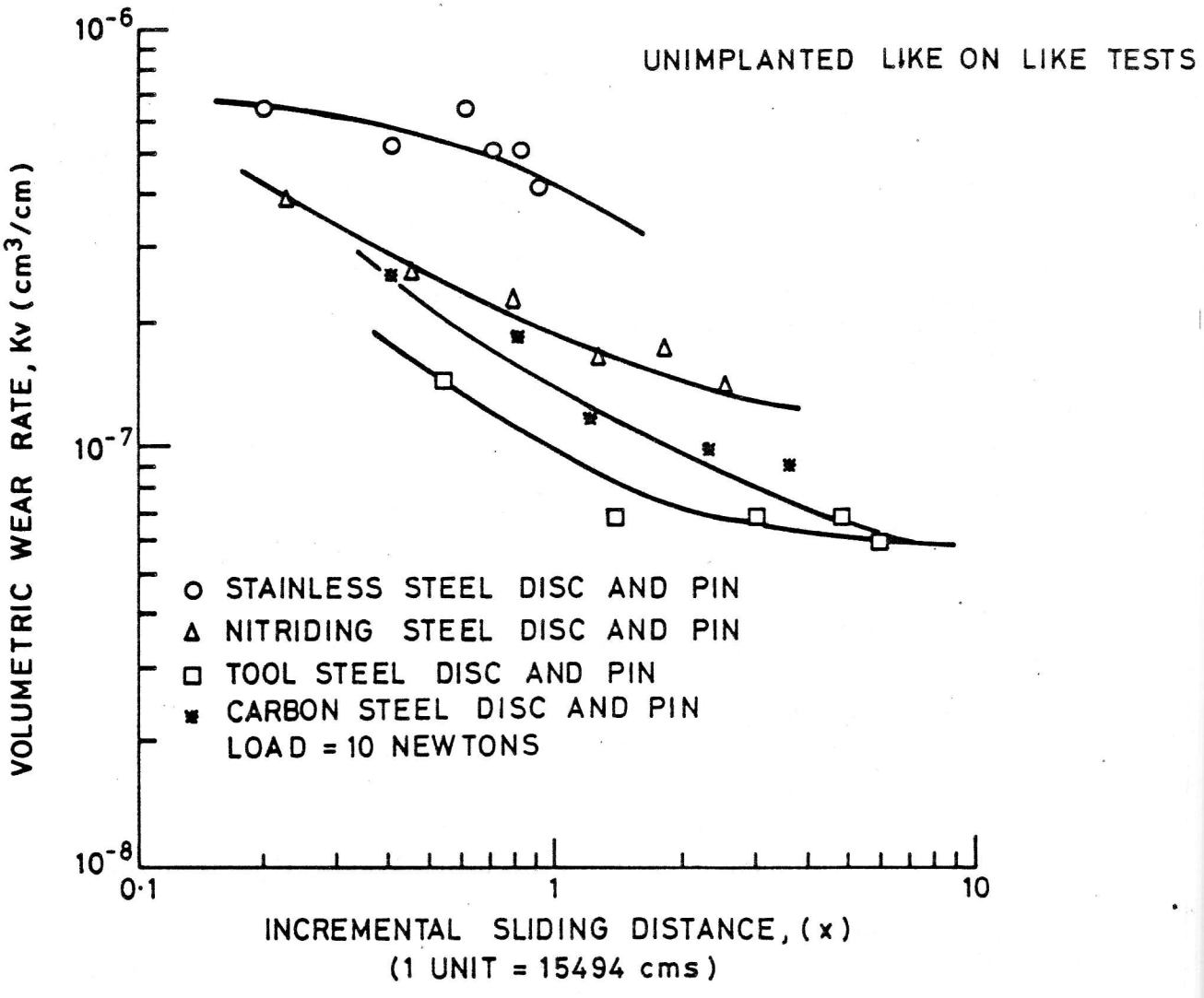

Fig. 14 Change in volumetric wear rate per unit contact area as a function of sliding distance for pin and disc tests on unimplanted En58B stainless steel, En40B nitriding steel, NsOH tool steel and En8 carbon steel discs lubricated with white spirit. Rotational speed = 600 r.p.m.

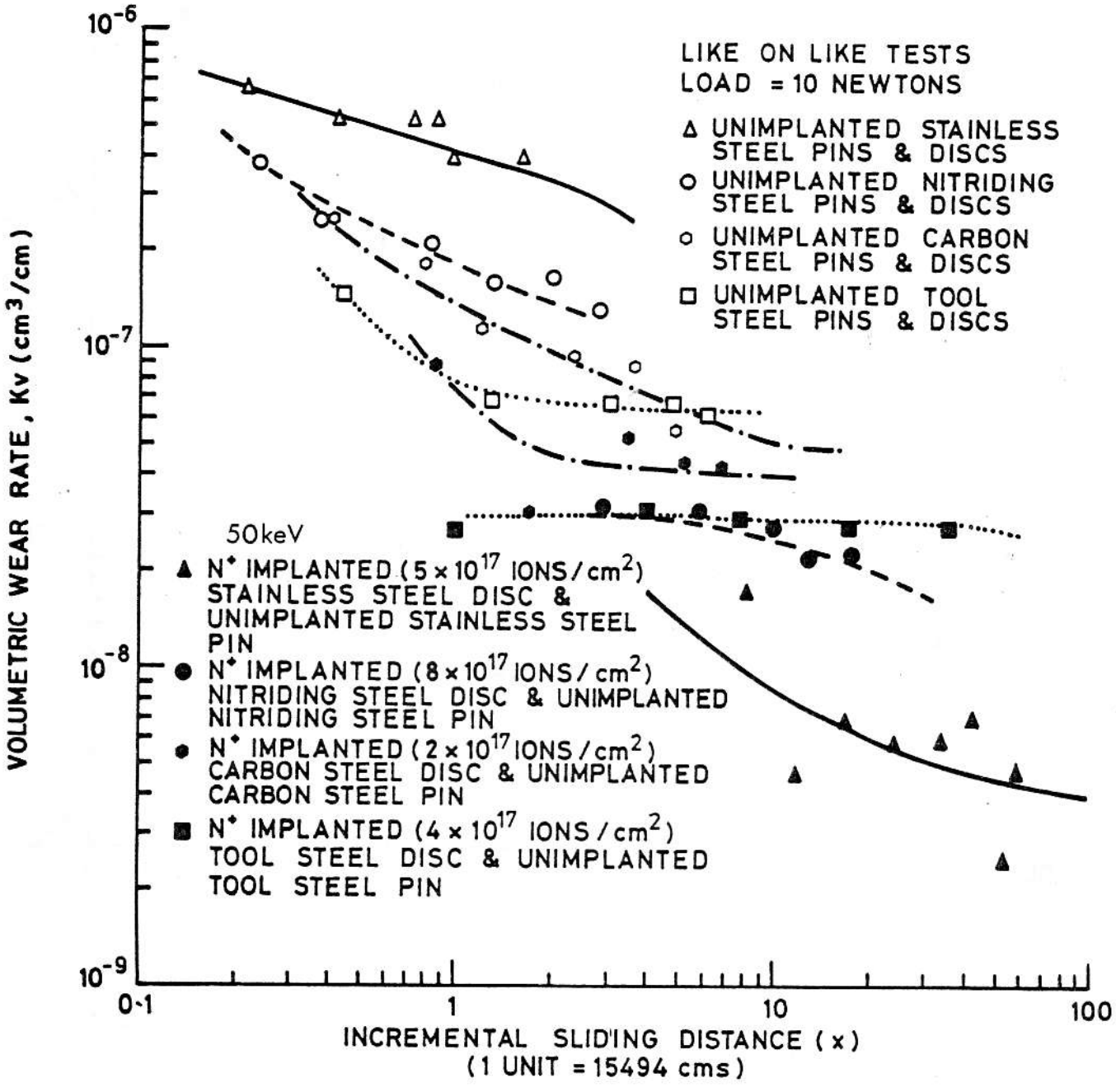

Fig. 15. As Fig. 14 except with N^+ implanted discs.

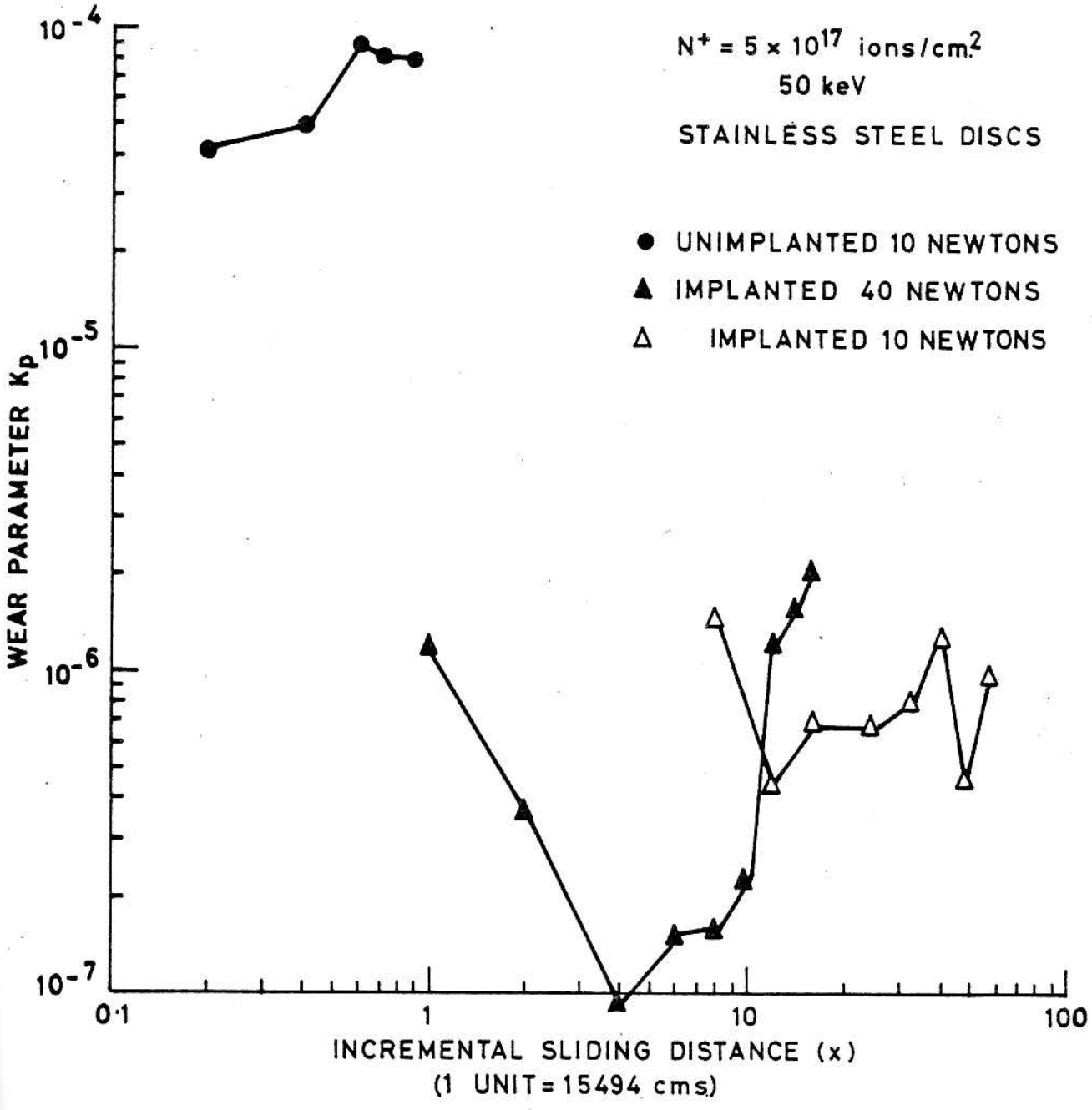

Fig. 16 Change in wear parameter Kp as a function of sliding distance for pin and disc tests on 50 keV N^+ implanted stainless steel discs lubricated with white spirit. Rotational speed = 600 r.p.m.

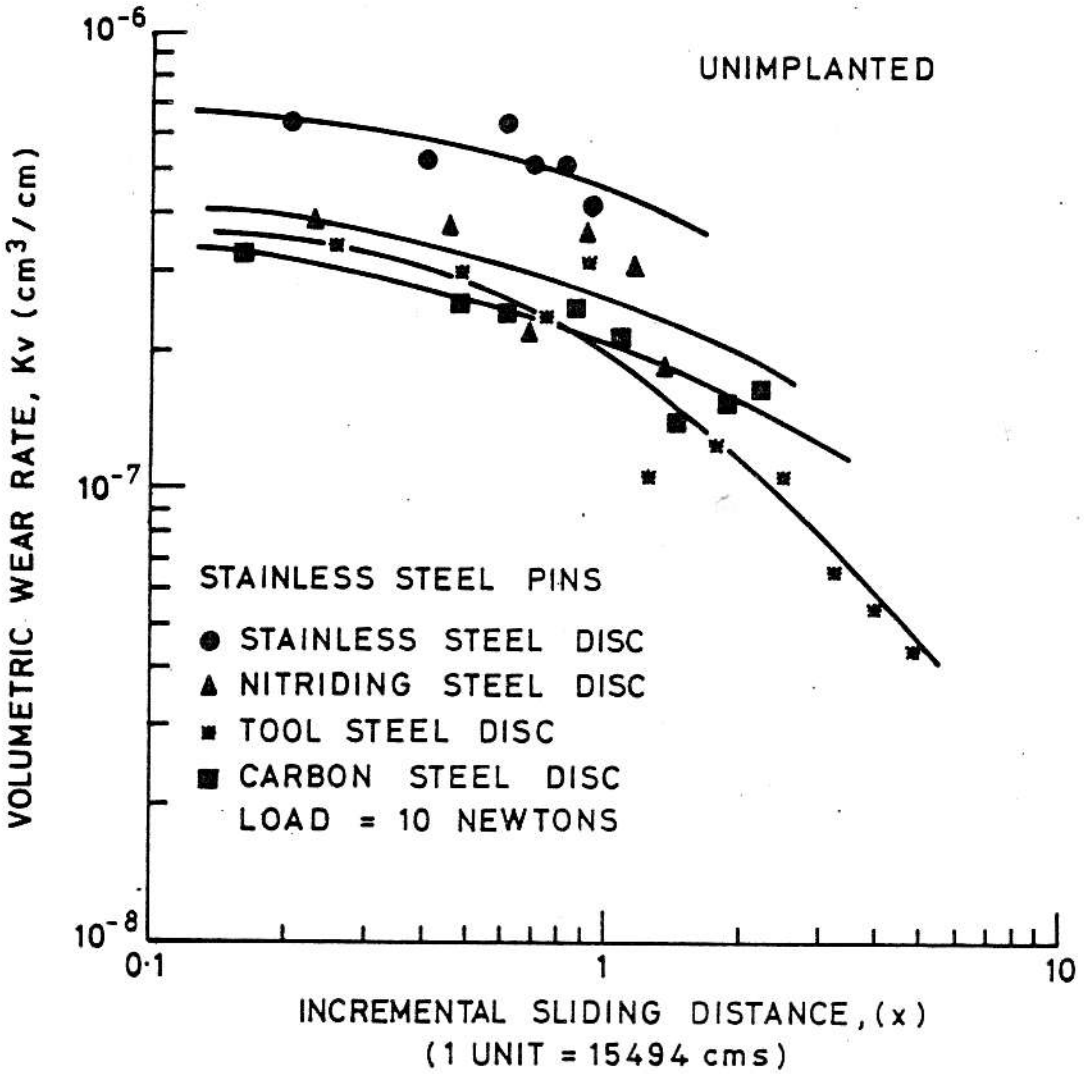

Fig. 17. Change in volumetric wear rate per unit contact area as a function of sliding distance for pin and disc tests on unimplanted En58B stainless steel, En40B nitriding steel, NSOH tool steel and En8 carbon steel discs lubricated with white spirit. Rotational speed = 600 r.p.m.

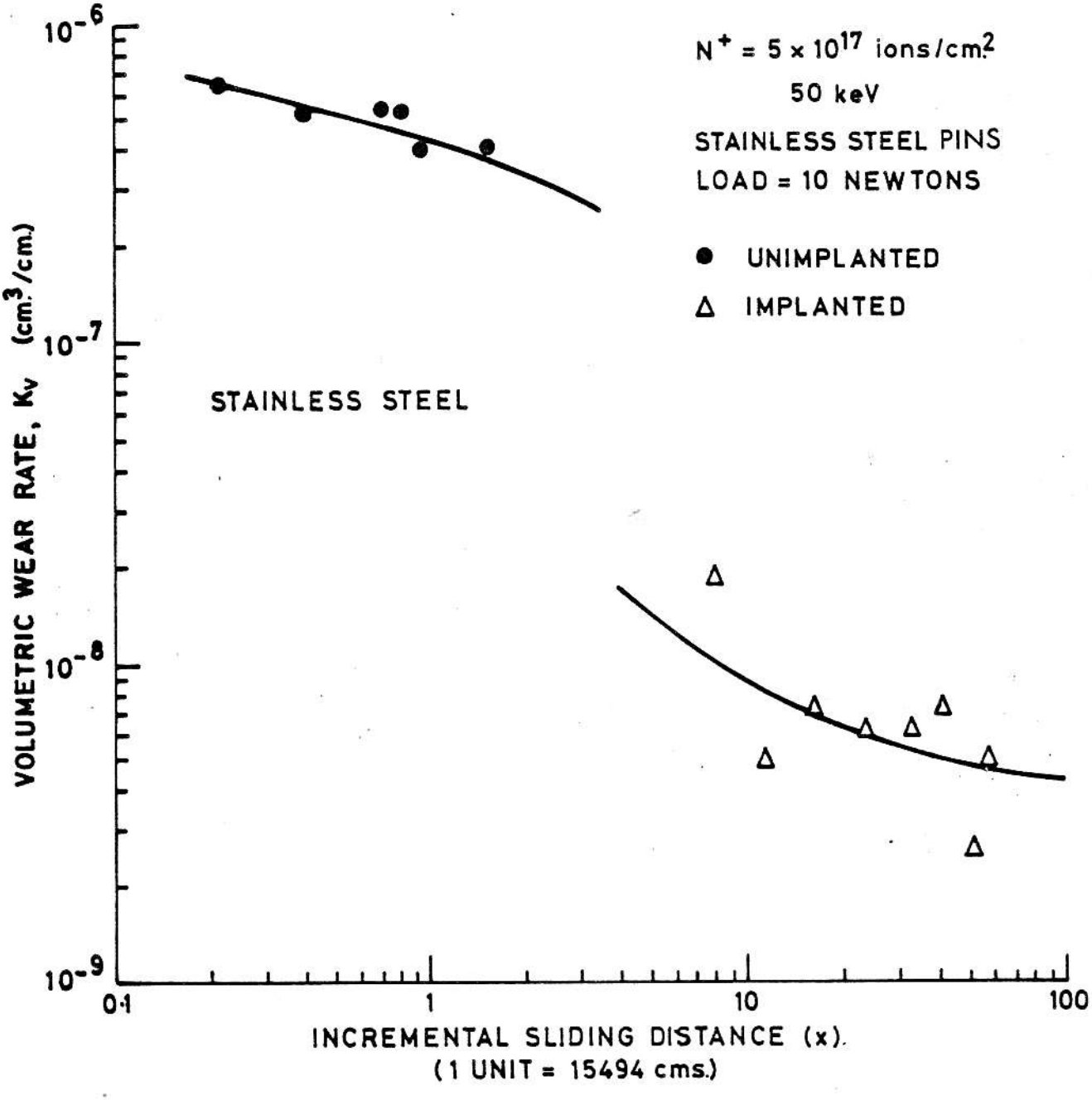

Fig. 18. Change in volumetric wear rate as a function of sliding distance for pin and disc tests on a 50 keV N^+ implanted En58B stainless steel disc lubricated with white spirit.

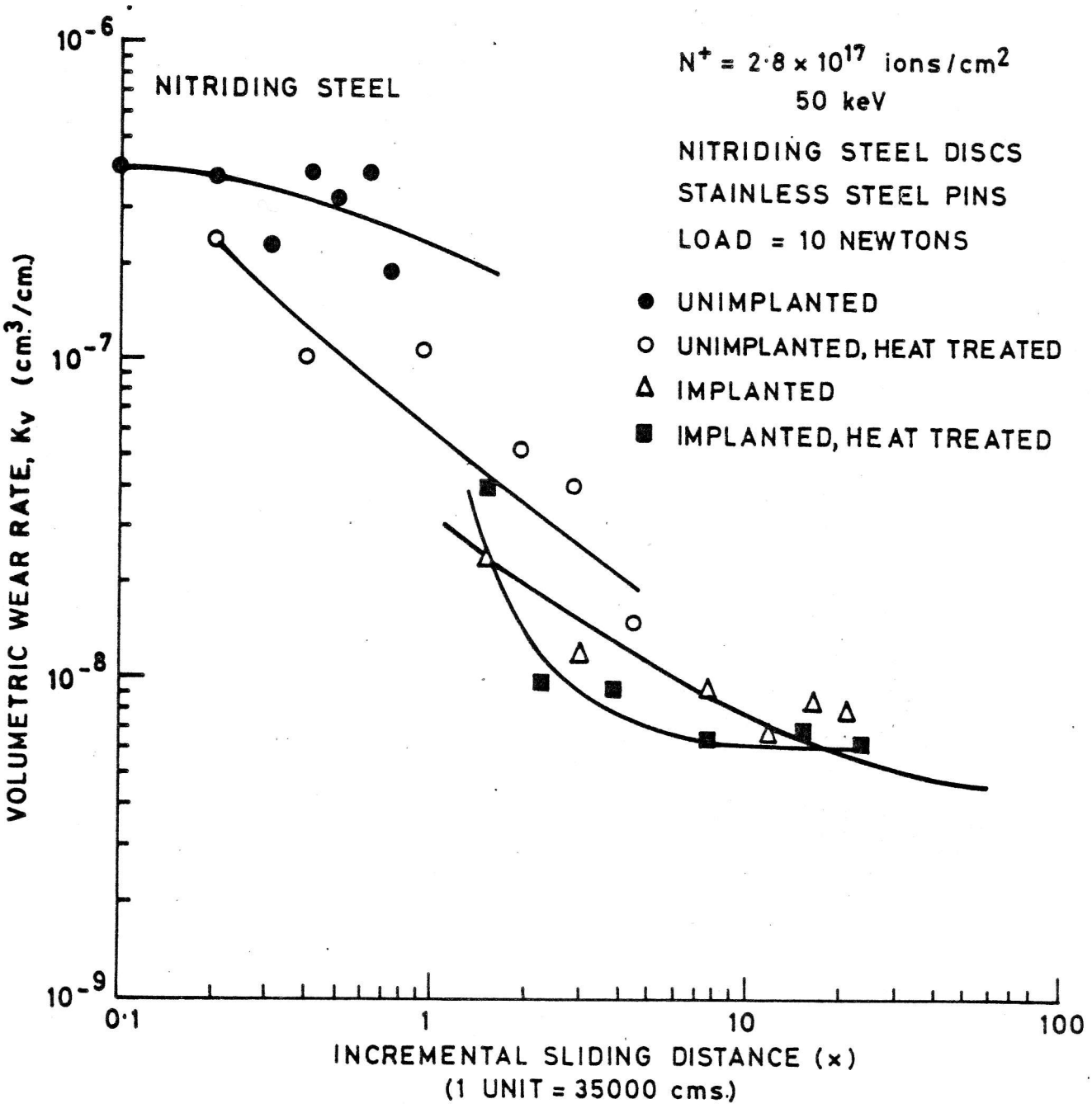

Fig. 19. As Fig. 18 but with En40B nitriding steel discs.

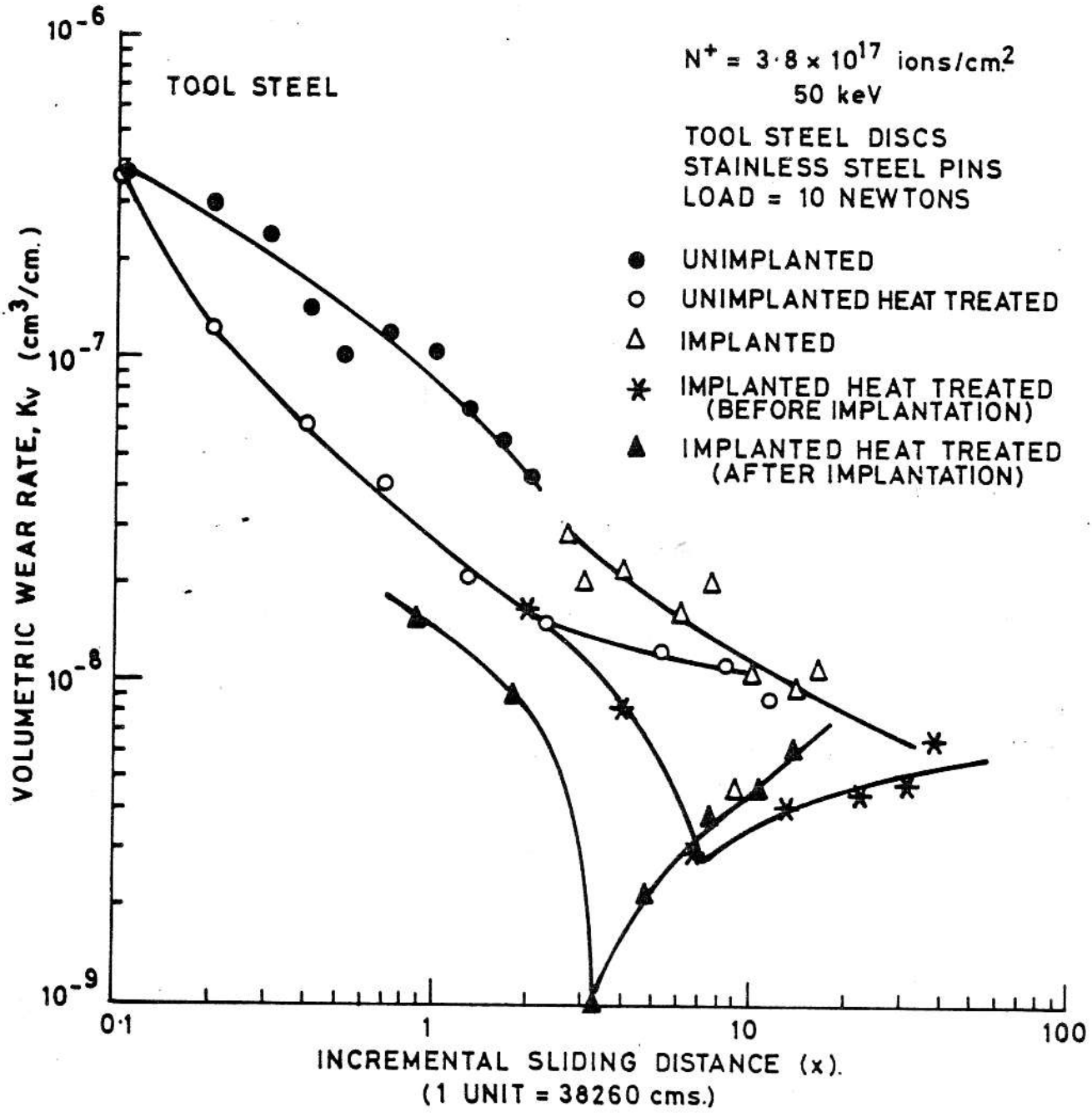

Fig. 20 As Fig. 18 but with NSOH tool steel discs.

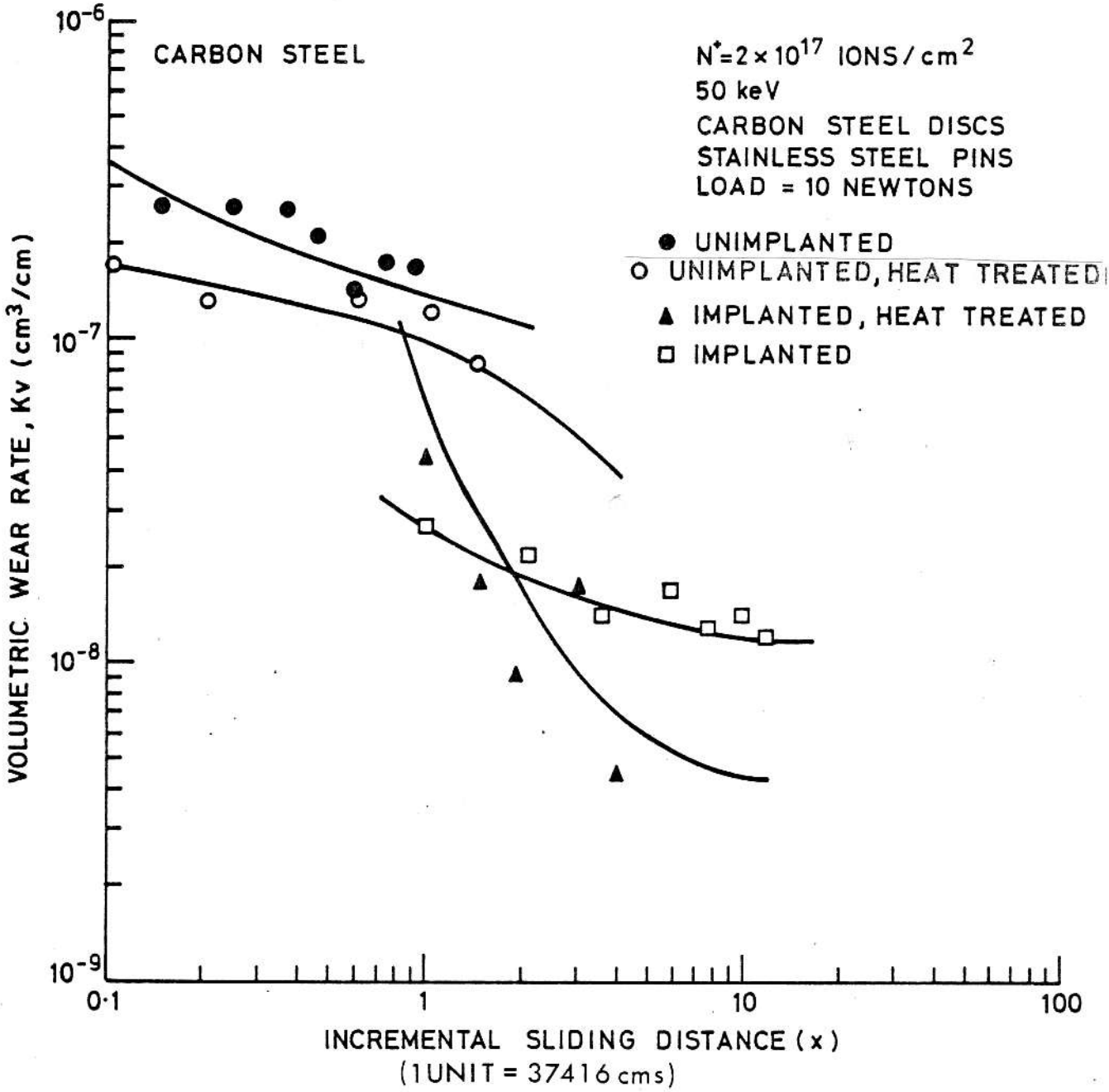

Fig. 21. As Fig. 18 but with En8 carbon steel discs.

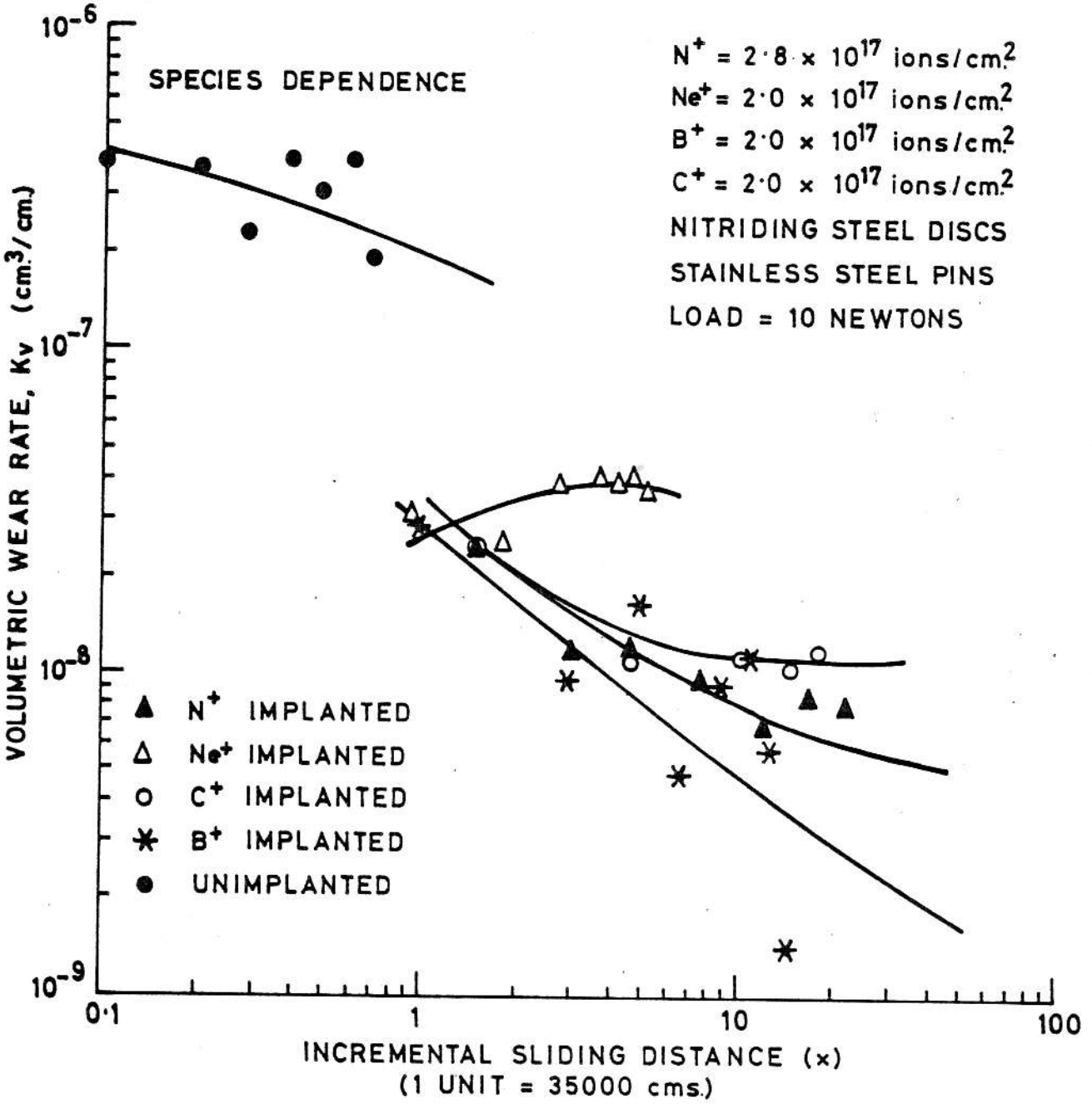

Fig. 22. As Fig. 18 but with 50 keV N^+ implanted, 40 keV C^+ implanted, 40 keV B^+ implanted and 50 keV Ne^+ implanted En40B nitriding steel discs.

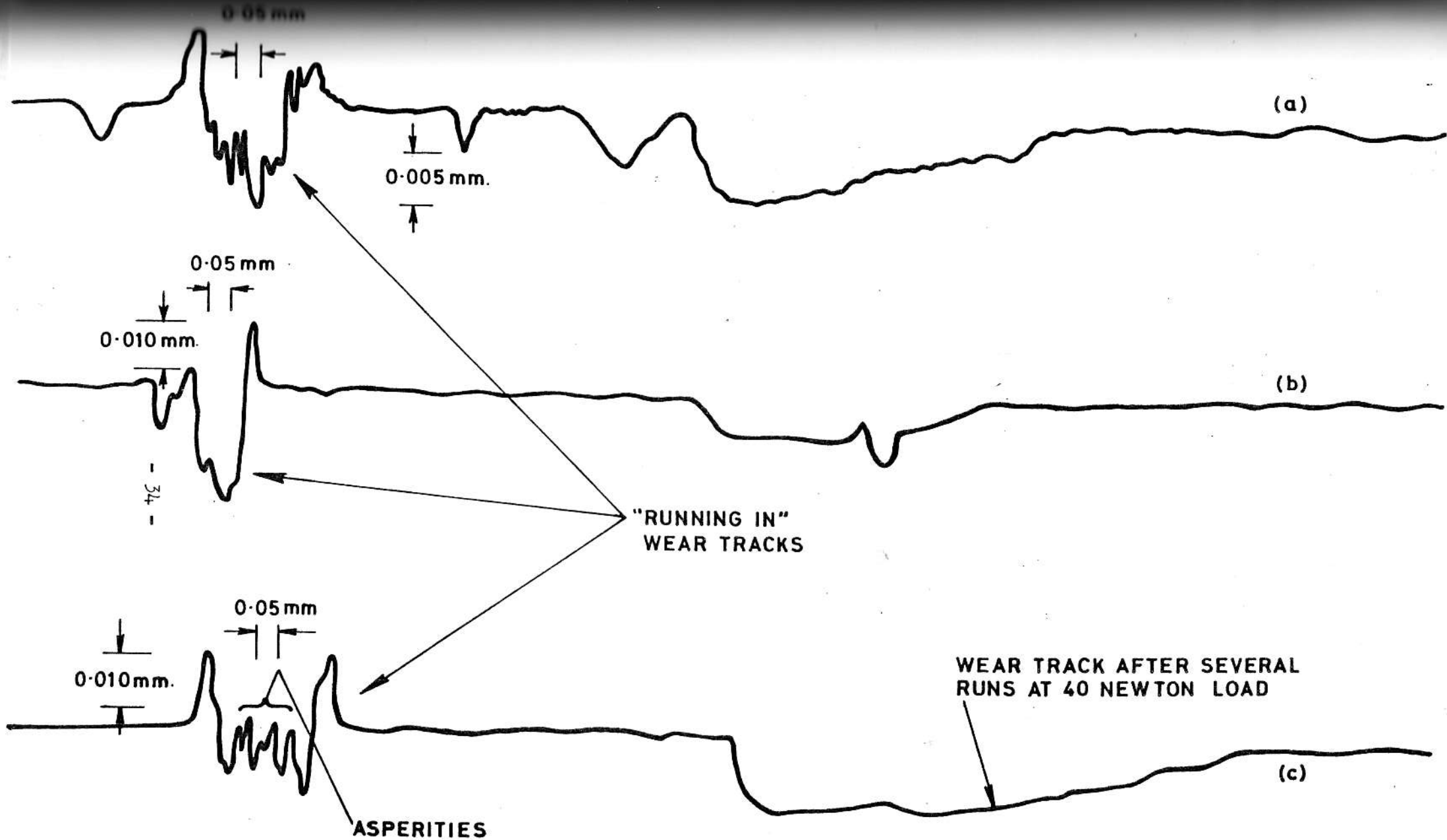

Fig. 23. Talysurf profiles of N^+ implanted, wear tested (a) stainless steel (b) nitriding steel and (c) tool steel discs.


0
20μ

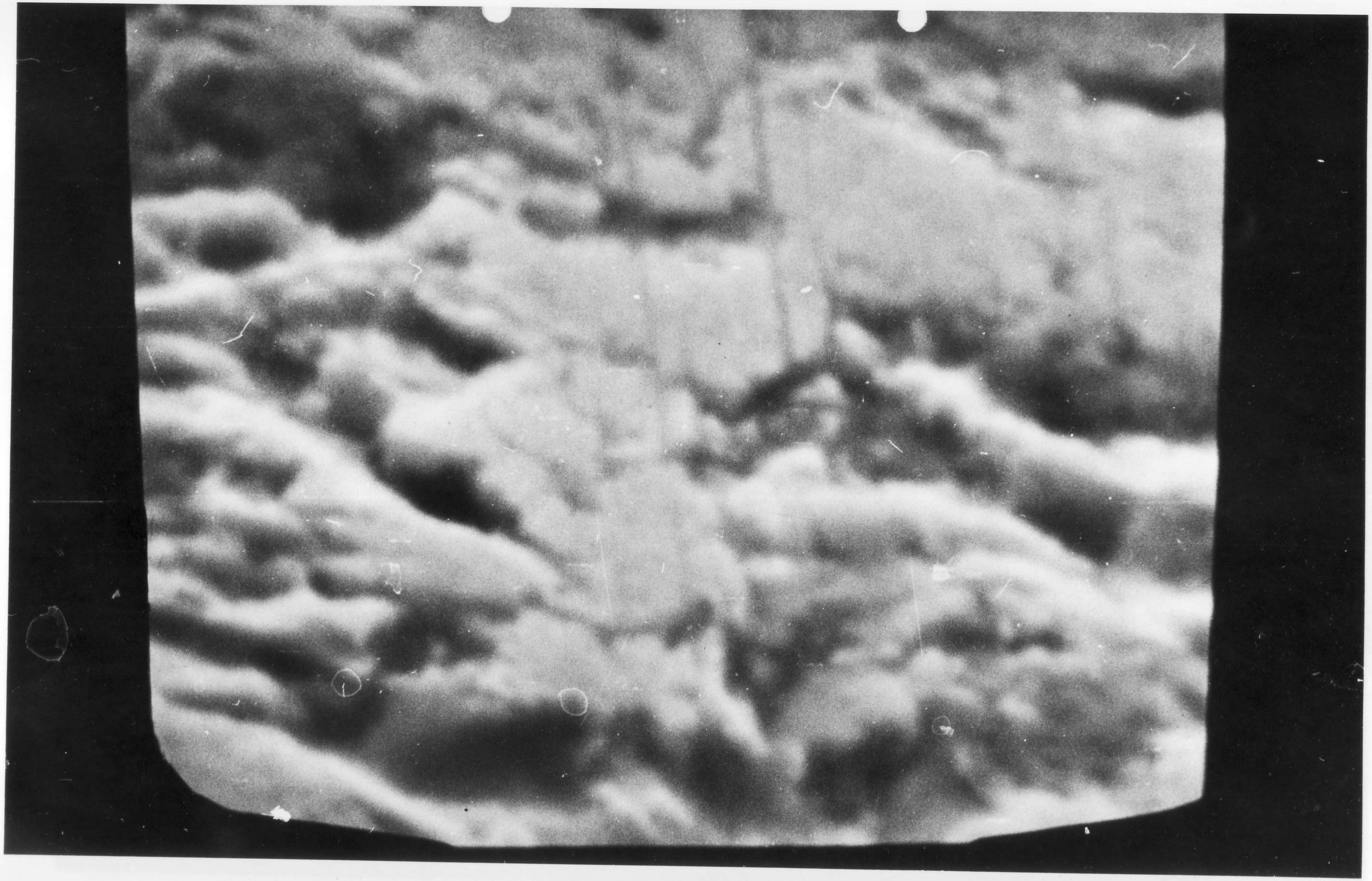

0 2m

0 40μ

IV

4.1 Unimplanted Like on Like Tests

Fig. 14 gives the relative wear performance of the four steels before implantation against unimplanted pins of the same steel. A stainless steel component in contact with another stainless steel component has been known for decades as a notorious combination in industry and its position on the wear graph is therefore not surprising. On the other hand, tool steel shows relatively good resistance to wear: by a factor of 4 it is better than stainless steel.

Plotted in this graph has been the volumetric wear rate against the incremental sliding distance. A particular line on the graph represents a run on a wear groove. This run is interrupted several times to measure the amount of material removed and the sliding distance between each interruption is known as the incremental sliding distance.

4.2 Like on Like Tests

Fig. 15 gives the corresponding results for the implanted discs, run against like pins, compared with similar runs for unimplanted discs. The most marked improvement is that for stainless steel, implanted to a dose of 5×10^{17} ions/cm^2 (solid black lines) an improvement by a factor of 14. The dashed, dotted, and dash-dotted lines represent similar - but not so marked - improvements for implanted nitriding steel, tool steel and carbon steel discs respectively (improvements of 6x, 2x and 3.5X at a sliding distance of 61976 cms).

4.3 Stainless steel on stainless steel Kp test

Fig. 16 shows a plot of the pin wear parameter Kp (defined in section 2.11) against the incremental sliding distance. As the pin wear parameter does not take into consideration change in contact area

there is no such downward trend with increase in sliding distance exhibited by the volumetric wear rate (K_v) plots. However, the results support the deductions from the K_v curves for stainless steel i.e. an improvement in wear resistance of 14 at a sliding distance of 61976 cms.

4.4 Unimplanted stainless steel tests

Fig. 17 and the following figures refer to discs of the four steels worn against unimplanted stainless steel pins. From Fig. 17 we obtain another comparison of the performances of the unimplanted steels. It is seen that the performances are worse because of the fact that stainless steel is a poor wear component.

4.5 Nitriding steel on stainless steel tests

In Fig. 19 we have compared the performance of implanted and heat treated En40B discs. One of the samples was heat treated and then implanted with nitrogen ions; however, this didn't improve the wear resistance significantly. Ion implantation, however, seems to be by a factor of 2 better than heat treatment for improving wear performance.

4.6 Tool steel on stainless steel tests

Fig. 20 compares the wear rate of tool steel (a) before implanting (b) after implanting with nitrogen ions (c) heat treating (d) heat treating then implanting and (e) Implanting then heat treating to see if the order of these two operations is important. Implanting only seems to have a small effect (an improvement of only ~1.1x); heat treating is better by a factor of two. Implanting and heat treating (both before and after implantation) collectively reduces the wear rate even more (up to 12x at a sliding distance of 46295 cms) but then this improvement breaks down, presumably because the implanted film has been broken through, as discussed later in this study.

4.7 Carbon steel on stainless steel tests

Fig. 21 reveals that ion implantation is a more successful method of improving wear resistance than heat treatment (7x compared to just 1.5x). Implanting and heat treating collectively only seems to produce a lower wear rate than just by implanting after a sliding distance of 74832 cms.

4.8 Investigation of the dependence of the wear properties on ion species for nitriding steel

In Fig. 22 we have compared wear performance of nitriding steel implanted with four different ions with the unimplanted steel. All implanted species give rise to similar wear properties (an improvement of about 6x) with the exception of neon whose effect breaks down after 63000 cms.

4.9 Wear Improvement Tables

Table 3

Unimplanted like on like Tests

j	$\frac{Kv}{Kv_j}$ st.steel (= improvement in wear)
Stainless steel disc + pin	1.0
Nitriding " " "	2.2 Sliding distance, x = 12395 cms
Tool " " "	4.2
Carbon " " "	2.9

Table 4

Like on like tests

j	$\frac{Kv_j \text{ unimpl.}}{Kv_j \text{ impl.}}$	
Stainless steel disc + pin	13.9	
Nitriding " " "	6.0	x = 61976 cms
Carbon " " "	1.8	
Tool " " "	3.4	

Table 5

Unimplanted disc on stainless steel pin tests

j	$\frac{Kv \text{ st.steel}}{Kv_j}$	
Stainless steel disc	1.0	
Nitriding " "	1.6	x = 12395 cms
Tool " "	1.4	
Carbon " "	1.4	

Table 6

En40B nitriding steel disc on stainless steel pin tests

j	$\frac{Kv \text{ unimpl.}}{Kv_j \text{ impl.}}$	
Unimplanted heat treated	7.3	
Implanted	12.5	x = 52500 cms
Implanted heat treated	12.5	

Table 7

NSOH tool steel disc on stainless steel pin tests

j	$\frac{Kv\ unimpl.}{Kv_j\ impl.}$	
Unimplanted heat treated	2.3	
Implanted	1.2	x = 80346 cms
Impl. heat treated (before impl.)	1.2	
" " " (after impl.)	5.2	

Table 8

En8 carbon steel disc on stainless steel pin tests

j	$\frac{Kv\ unimpl.}{Kv_j\ impl.}$	
Unimplanted heat treated	1.6	
Implanted	5.6	x = 56124 cms
Implanted heat treated	5.5	

Table 9

Species dependence tests

j	$\frac{Kv\ unimpl.}{Kv_j\ impl.}$	
N^+	14.5	
Ne^+	11.7	x = 52500 cms
C^+	14.5	
B^+	16.7	

4.10. Nuclear reaction analysis $^{14}_{7}N(d,\alpha)^{12}_{6}C$ alpha particle spectra

Figs. 9 and 10 show the alpha particle spectra for two of the samples analysed - nitrogen implanted stainless and nitriding steels respectively. The x-axis is a measure of the energy of the particle emitted and the y-axis a measure of the number of particles at that energy. The α_o peak corresponds to an energy of about 10MeV. The height of this peak is compared with the height of a standard, for example silicon nitride, to obtain the amount of nitrogen present. An interesting and important part of this work was a comparison of the height of the peak at the pit of a wear groove with that at the surface of an unworn region for tool steel (section 5).

5. Discussion

The wear improvement tables show quite clearly that for all implanted discs there is an improvement in wear resistance, ranging from a factor of 1.2 for tool steel wearing against stainless steel to 14 for stainless steel against stainless steel. One could question the reliability of the results though: For instance, it can be seen from the figures that the unimplanted regions and implanted regions generally only overlap to a small extent - this is illustrated clearly in the stainless steel figures (16 and 18). The overlap is small because of the fact that it takes much larger sliding distances to remove equivalent amounts of material, coupled to the restraints on the size of the flat (0.2 - 0.5 mm) mentioned in section 3.3. However, by comparing the wear rate for a given sliding distance in the region of overlap, this problem can be overcome.

From the figures it can be seen that, aside from implantation, wear properties improve with increasing sliding distance. This can be accounted for by the increase in the contact area causing the normal stress - and hence the wear rate - to be reduced.

The problem now is to try and account for the improvement in wear resistance caused by ion implantation. Since the wear tests were carried out under fully lubricated conditions, it is necessary to take into account the effects of asperity deformation and strength on the load bearing properties of the white spirit film also. Johnson et al.[8] (see also Hartley[6] for a review of this work) have shown that the pressure on the asperities is related to the film thickness by

$$\frac{p_f}{p_o} = \left(\frac{h_o}{h}\right)^{6.3} \qquad \ldots\ldots (8)$$

where p_f is the fluid pressure, p_o the total pressure, h and h_o film thicknesses for rough and smooth surfaces. Thus by the smoothing out of asperities during wear the stress on the film increases with a corresponding decrease in effective film thickness. Now ion implantation, as mentioned in section 2.2, has the effect of hardening the surface of the asperities so that when contact occurs small equiaxed particles are broken off to produce a net smoothing of the surface. The reduction of h (eqn. 8) during wear due to smoothing causes the pressure in the film to rise sharply and the contact points support less load, giving improved wear resistance.

Thus, since the pin and disc are in intermittent contact, the effective smoothing of one surface combined with a more efficient lubricant distribution between the two surfaces results in a reduction of the wear rate for this tribological couple. However, from the talysurf profiles (Fig. 23) it is quite clear that the depth of the wear grooves is by a factor of up to a thousand deeper than the ion range predicted by the LSS theory (section 2.2) - and the wear improvement holds out to at least the groove depths in most samples - the exceptions being the neon implanted En40B steel (Fig. 22) and the nitrogen implanted heat treated tool steel discs (Fig. 18) all run against stainless steel pins.

The depth profiles of nitrogen (Figs. 10 and 11) in the En58B stainless and En40B nitriding steel N^+ implanted discs show that the distribution is much deeper and is far from Gaussian as predicted by the LSS theory. The En58B stainless steel disc has a nitrogen peak at approximately 1200Å (14% nitrogen) and tails off to a negligible value at about 4000Å. In the En40B nitriding steel sample there is no such clearly defined peak however - there is more of a flat distribution

(max. 5% nitrogen) truncated at the surface. The distribution tailed off very gradually so that there was still a considerable amount left (2.5%) at 7000Å. Also included in these plots are depth distributions for carbon, chromium, nickel and iron to see if the different amounts of these elements in each sample could be related to the different nitrogen profiles. However, any direct comparison cannot be taken too literally as the stainless steel had received 1.8 times more nitrogen ions. This was an unfortunate consequence of the different rates of emission of secondary electrons from the different steels during implantation thus affecting the reading of the beam current to differing degrees. This would, on the other hand, merely effect the size of the peak as the LSS theory predicts that the range is dependent on ion energy rather than dose.

X-ray photoelectron spectroscopy also revealed that there was far more free than chemically combined nitrogen. This results in higher diffusion coefficients. During the implantation process, local temperature rises are between 250 and 300°C.[10] Now Hartley and Longworth[9] have found from Mossbauer spectroscopy studies that nitrogen becomes mobile at 275°C - this lies within the implantation temperature range. The compressive stress caused by implantation which we mentioned in section 2.2 also increases the diffusivity by factors of three to five (Dearnaley and Hartley[11]). Thus these two effects could account for the deeper profiles.

Even so, 7000Å is still nearly a hundred times shallower than the depth of the grooves so there must be some other mechanism or mechanisms causing the region of ion damage to move in with the wear groove. This

could be related to the compressive stress during implantation i.e. a movement of ions induced by the load stress applied normally. This stress gradient hypothesis has been investigated by J. Charles at Cambridge who found however that this effect is negligible.

C.P. Flynn[12] discusses the possibility of thermal migration of the nitrogen ions into the bulk of the steel as a result of local frictional heating during the wear process. (nitrogen in steel, we recall, becomes mobile at 275°C). Unfortunately there has been no success thus far in measuring the local temperature rise. However, in this study nuclear reaction analyses were performed on the pit of the wear groove and revealed that there was 30% of the surface nitrogen still present. This is consistent with the inward movement of nitrogen during wearing. Since the Charles team at Cambridge found no reason for migration under the influence of a stress gradient, it seems likely that the frictional heating is responsible for the movement.

It is also interesting to note that the run in wear groove (Fig. 23(c)), run for ~10,000 cm is of the same order of depth as the 40N groove, run for ~1,000 cm. This is not necessarily due to a hardening of the groove pit relative to its sides: Due to the centripetal force caused by the motion of the disc, wear particles tend to be thrown onto the outer side of the groove and hence abrasive wear tends to occur here. Another factor is that wearing of the groove was successively interrupted and the pin removed for pin measurements and then replaced back in the groove - not necessarily in exactly the same position as before.

The neon implanted En40B sample - nominally* implanted to a dose

---

*Unfortunately there is no nuclear reaction analysis available for neon to check the dose.

of 2 x 10^{17} ions/cm^2 showed very little retention of neon from the XPS data (Fig. 13). With a peak signal of 1.1% there was virtually no neon (which is insoluble in steel) present deeper than 300Å. One could therefore correlate this with the breakdown to wear resistance (Fig. 22) as mentioned above. The En40B samples implanted with boron, carbon and nitrogen ions showed no signs of breakdown however and exhibited similar wear properties with the boron implanted sample the best. Thus wear improvement seems to be little dependent on the chemical nature of the implanted species but rather their size and solubility.

Finally we compare ion implantation with heat treatment as a method of improving wear resistance, recalling that the former does not affect the bulk properties of a sample. Fig. 19 and Table 6 reveal that for En40B nitriding steel, implantation of one component has twice the effect of heat treatment whereas implanting heat treated samples has little improvement on just implanting. With tool steel however (Fig. 20 and Table 7) one can deduce that heat treatment has twice the effect of ion implantation whereas heat treating both before and after implantation improves the wear properties even more until the hardened film referred to above is broken through. Implantation appears to be better than heat treatment by a factor of 3.5 for En8 carbon steel (Fig. 21 and Table 8) but the implanted heat treated samples showed better properties at higher sliding distances.

6. Conclusions

It has been shown in this study that, for En58B stainless steel, N.S.O.H. tool steel, En40B nitriding steel and En8 carbon steel:

(i) Ion implantation of one component of a tribological couple under lubricated conditions, can increase the wear resistance of steels by over an order of magnitude. The exact figure depends on the wearing

component, the nature of the ion implanted and the sliding distance.

(ii) Implantation is a viable alternative to heat treatment; in all cases bulk properties are not affected, and the actual improvement is better except for tool steel.

(iii) Implanting and heat treating collectively shows only a slight improvement on just implanting alone, with the exception of tool steel, up to a sliding distance of approximately 46 metres.

(iv) The chemical nature of the ion species is relatively unimportant, apart from the size and the solubility in the steel.

(v) Finally, the results have also supported existing theories on the mechanisms of wear improvement caused by ion implantation and have provided a sound framework for further work in this field.

7. Further Work

1. Determination of the local temperature rise during wearing. This would check the validity of our assumption that the rise is sufficient to enable nitrogen to diffuse into the sample.

2. More work with different insoluble ions and also molecular species would check our deductions from the neon data.

3. More work using different steels would check the generality of all our conclusions.

4. Dose dependence studies on a wide range of steels - at present only En40B nitriding steel has been examined after implanting with 30keV nitrogen ions,[6] (Fig 8). The assumption that these properties are general, as made in this study, would then be justified or otherwise.

5. Although the bulk properties of all the steels are unaffected by implantation, surface properties are; for stainless steel this could

be critical i.e. implanting could remove its "stainless" properties. Thus corrosion tests on implanted stainless steel would be very useful.

6. Finally, the effects of implanting both components of a tribological couple, i.e. disc and pin , has yet to be studied.

8. Acknowledgements

I would like to take this opportunity to thanking Dr. N. Hartley, Dr. G. Dearnaley, Mr. R. Watkins and Dr. J. Riviere for their encouragement and many useful discussions and also Mr. G. Proctor for operating the oscillating electron ion source. I am also grateful to the Atomic Energy Research Establishment, Harwell, for giving me permission to use their equipment. This work was sponsored by a Science Research Council Studentship.

Appendix

Appendix I : Sputtering Loss

According to Bett and Charlesworth[7] the depth of material removed during implantation , d , is given by

$$d = \frac{D.S}{N} \qquad \ldots\ldots\ldots\ldots\ldots\ldots\ldots\ldots \quad (A1)$$

where D is the dose implanted (ions/ cm^2), S is the sputtering coefficient and N the atomic density of the material.

The maximum dose worth implanting into the material is shown to be given by

$$D_\infty = \frac{2.N.\overline{Rp}}{S} \qquad \ldots\ldots\ldots\ldots\ldots\ldots\ldots\ldots \quad (A2)$$

where $\overline{Rp}$ (the ion range) $\sim$ 550 A

$N \sim 8 \times 10^{22}$ atoms / cm^3

$S = 1.53$

The $\overline{Rp}$ and S values are those for an implantation energy of 50 keV. This gives the maximum dose as $D_\infty = 5.75 \times 10^{17}$ ions/ cm^2.

Appendix II : The Accuracy of the Wear Measurements

Maximum error in diameter of pin flat = 1.3 % ,

" " " area " " " = 2.6 %,

" " " volume " " " = 3.9 % ,

" " " sliding distance, x, = 1 % .

Thus the maximum possible error in the volumetric wear rate

= 2.6 + 3.9 + 1 = $\pm$ 7.5 %.

Appendix III : The Accuracy of the Depth Profiles

As mentioned in the discussion, these results cannot be taken too literally because of the different sputtering coefficients of the atomic species, i.e., those with lower coefficients tend to build up relative to those of higher coefficients the deeper we probe into the surface. This is best illustrated by the carbon profiles in Figs 11 and 12: The solubility of carbon in steel is less than 0.2 %, thus the 14% average value from the profiles is either due to this effect or to the fact that there was a lot of undissolved carbon present before the analyses. Alternatively there could have been a lot of surface contamination resulting from residual lubricant left on the surface, despite cleaning thoroughly. Fortunately though nitrogen has a high sputtering coefficient so the nitrogen profiles are reasonably reliable.

Appendix IV : Electron micrographs of the wear grooves

Plate II shows half of a segment of a run in wear groove and Plate III shows about a tenth of a segment of a wear groove after several runs at a pin load of 40 Newtons, run for about ten times the distance of that in Plate II. It can be seen that the grooves are much more shallower and difficult to resolve for the track in III - despite the greater magnification. This is because the asperities on the pin have been worn down and hence do not create such deep furrows as in II. In fact this is exactly what we found from the talysurf profiles (Fig 23). Plate IV shows an interesting view of a wear groove formed during unlubricated wear ("severe wear"). The rounded edge of the platelet implies that melting temperature was reached during wearing.

Bibliography

1. MOORE, D.F., Principles and Applications of Tribology, Pergamon (1975)
2. SARKAR, A.D., Wear of Metals, Pergamon (1976)
3. HARTLEY, N.E.W., Surface stresses in Ion Implanted steel, AERE-R 7842 (1974)
4. LINDHARD, J., SCHARFF, M., and SCHIØTT, H.E., Kgl. Danske Vid. Selsk. Matt. - Fys. Medd. 33 No. 14, (1963)
5. The British Standards Steels Book
6. HARTLEY, N.E.W., Tribological Effects in Ion Implanted Metals, AERE- R8171 (1975)
7. BETT, R., and CHARLESWORTH, J.P., Estimation of Ion-Implanted impurity distribution in cases involving high dose or sputtering ratio, AERE-R7052
8. JOHNSON, K.L., GREENWOOD, J.A. and POON, S.Y., Wear 19 , 91 (1972)
9. LONGWORTH, G. and HARTLEY, N.E.W., Mossbaur effect study of nitrogen implanted iron foils, AERE (to be published)
10. DEARNALEY,G., FREEMAN,J.H., NELSON,R.S. and STEPHEN,J.,Ion Implantation, P.423, North-Holland, (1973)
11. DEARNALEY, G., HARTLEY, N.E.W., New Uses of Ion Implantation, AERE-R 8562 (1976)
12. FLYNN, C.P., Point Defects and Diffusion, O.U.P., (1972)